tion potency agreed well with observed tumor incidence in the oral bioassays. This correspondence across routes based on metabolized dose contrasted with the apparently higher potency of VC by the oral route when the comparison was based on 'inhaled' vs. 'ingested' dose in milligrams per kilogram per day.

Chen and Blancato (1989) also used the PBPK model to calculate the human inhalation potency for VC-induced liver cancer based on epidemiological data (Fox and Collier, 1977). Using the same pharmacokinetic dose measure (mg metabolized kg^{-1} day^{-1}), the inhalation potency estimated from epidemiological data (3.8×10^{-3} ppm^{-1}) was essentially identical to the potency estimated from rat inhalation data ($1.7–3.7 \times 10^{-3}$ ppm^{-1}), using body weight scaling (i.e. without applying the BSA adjustment). However, a second, more complicated comparison performed in the same analysis, which involved time-to-tumor modeling, suggested that the BSA adjustment might be necessary to accurately predict lifetime-exposure human cancer fatality from animal incidence data.

More recently, a PBPK model of VC was developed by Reitz et al. (1996) and applied to compare cancer potency in mice, rats, and humans. The structure of the model was similar to that of Chen and Blancato (1989), providing a description of parent chemical kinetics and total metabolism based on the styrene model of Ramsey and Andersen (1984). Metabolism of VC was modeled with a single saturable pathway, and the kinetic constants were estimated from fitting of closed chamber gas uptake studies with rats. The model was then validated against data on total metabolism in the rat (Watanabe et al., 1976b), gas uptake data in the mouse, and inhalation data in the human (Baretta et al., 1969). The model was used to calculate total metabolism of VC as the dose metric in a carcinogenic risk assessment. Based on the rat inhalation bioassay of Maltoni et al. (1981, 1984), and using the linearized multistage model, they estimated that lifetime continuous human exposure to 1.75 $\mu g/m^3$ VC is associated with an increased lifetime risk of one in a million. This estimate equates to a lifetime risk of approximately 1.5×10^{-3} ppm^{-1}, in good agreement with the results of Chen and Blancato (1989). The potency estimates from rats were then shown to be consistent with tumor incidence data in mice and humans when the pharmacokinetic dose metric was used.

2. Pharmacokinetics and metabolism of VC

Numerous studies on the pharmacokinetics and metabolism of VC have been conducted, with the majority of these studies conducted in rats (Withey, 1976; Hefner et al., 1975; Guengerich and Watanabe, 1979; Bolt et al., 1976, 1977; Watanabe et al., 1976a,b, 1978, Jedrychowski et al., 1984, 1985; Tarkowski et al., 1980). A simplified diagram of the metabolism of VC is shown in Fig. 1. The primary route of metabolism of VC is by the action of the mixed function oxidase (MFO) system, now referred to as Cytochrome P450 or CYP, on VC to form chloroethylene oxide (Bolt et al., 1977; Plugge and Safe, 1977). Chloroethylene oxide (CEO) is a highly reactive, short-lived epoxide that rapidly rearranges to form chloroacetaldehyde (CAA), a reactive α-halocarbonyl compound; this conversion can also be catalyzed by epoxide hydrolase (Pessayre et al., 1979).

The main detoxification of these two metabolites is conjugation binding with glutathione (Jedrychowski et al., 1985; Leibman, 1977; Tarkowski et al., 1980). This hypothesis is supported by the observation of decreased non-protein sulfhydryl concentrations at high VC exposure concentrations (Jedrychowski et al., 1985; Tarkowski et al., 1980), as well as by the excretion of glutathione (GSH) conjugated metabolites in the urine, observed in rats following exposure to VC (Watanabe et al., 1976c; Hefner et al., 1975). CAA may also combine directly or enzymatically via glutathione transferase (GST) with GSH to form *S*-formylmethylglutathione. The GSH conjugates are then subject to hydrolysis resulting in excretion of cysteine conjugates in the urine (Hefner et al., 1975). Two of the three major urinary metabolites of VC in rats have been identified as *N*-acetyl-*S*-(2-hydroxyethyl)cysteine and thiodiglycolic acid (Watanabe et al., 1976b).

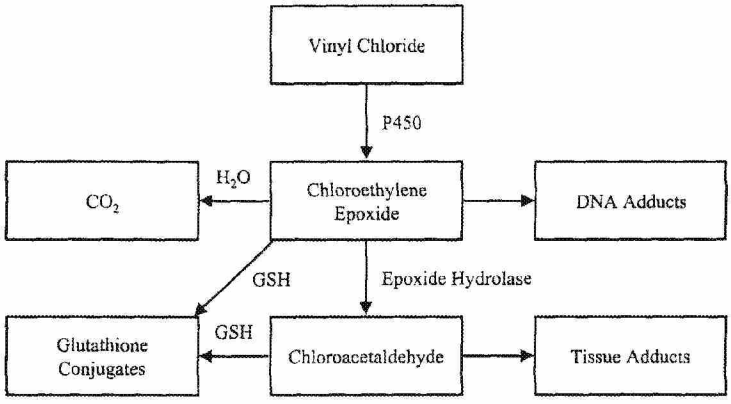

Fig. 1. Diagram of the metabolism of vinyl chloride (VC). Abbreviations: P450, Cytochrome P450 (CYP); GSH, glutathione.

Based on the elimination of VC observed following administration by various routes of exposure, the metabolism of VC appears to be a dose-dependent, saturable process (Green and Hathway, 1975; Bolt, 1978; Hefner et al., 1975; Gehring et al., 1977, 1978). Following exposure via oral or inhalation routes to low doses of VC, metabolites are excreted primarily in the urine. However, once the saturation point for metabolism is reached, VC is eliminated via other routes, primarily exhalation of the parent compound (Gehring et al., 1977; Watanabe et al., 1976b; Watanabe and Gehring, 1976). The route of elimination of VC also depends on the route of administration, with urinary excretion favored more following oral or intraperitoneal administration, indicating a first-pass effect due to liver metabolism (Bolt, 1978).

The specific isozymes of the P450 system involved in the metabolism of VC have not yet been unequivocally established. However, it is clear from both in vitro and in vivo studies that several isozymes can play a role. High affinity, low capacity oxidation by CYP 2E1 is probably responsible for essentially the entire metabolism of VC at low concentrations in uninduced animals and humans (Guengerich et al., 1991). There is also evidence for a significant increase in metabolism in animals pretreated with phenobarbital (Ivanetich et al., 1977), suggesting that CYP 2B1 also metabolize VC. At high concentrations in vivo, the metabolism of VC in rats leads to a destruction of P450 enzyme (Reynolds et al., 1975), which is greatly enhanced in phenobarbital — or Arochlor — induced animals (Arochlor induces CYP 1A2). The loss of P450 has been suggested to result from the production of reactive intermediates during the metabolism of VC (Guengerich and Strickland, 1977), and is inhibited by GSH in vitro (Ivanetich et al., 1977). Induction of P450 by phenobarbital or Arochlor was also necessary to produce acute hepatotoxicity from VC in rats (Jaeger et al., 1977).

The contribution of several P450 isozymes to the metabolism of the related compound trichloroethylene has been studied in the male Wistar rat and male B6C3F1 mouse (Nakajima et al., 1993). Using monoclonal antibodies specific to each isozyme, the investigators were able to determine that: (1) CYP2E1 contributes more to the metabolism of TCE in mice than in rats; (2) CYP2C11/6 contributes more to the metabolism of TCE in rats than in mice (CYP2C11/6 is a constitutive, non-inducible isozyme present only in male rodents); (3) CYP1A1/2 contributes to the uninduced metabolism of TCE in mice but not in rats; and (4) CYP2B1 does not contribute to the metabolism of TCE in naive animals of either species.

Summarizing the above observations, it appears that at low concentrations the metabolism of VC is primarily due to CYP2E1, but that at higher concentrations, where CYP2E1 becomes capacity-limited, other isozymes may contribute to its metabolism. The extent of this higher-capacity metabolism is likely to vary across animal species, strain, and sex. To the extent that such higher capacity, lower affinity metabolism (referred to in future as 'non-2E1' metabolism) may be important in conducting a risk assessment for VC, it will have to be characterized separately for each species, strain, and sex of interest. From a pharmacokinetic modeling perspective, non-2E1 metabolism would be handled as a second saturable metabolic pathway with a larger value for the Michaelis–Menten constant (KM). For example, it has been demonstrated that the metabolism of the related compound, vinyl bromide, is best described with two distinct saturable pathways having different affinities (Gargas and Andersen, 1982). Of major importance for human risk assessment, some of the low-affinity, high capacity constitutive (2C11/6) and inducible (2B1/2) P450 isozymes in the rodent may have no human correspondents (Guengerich, 1987).

2.1. Pharmacokinetic modeling of VC

The pharmacokinetic models that have previously been used in risk assessments for VC (Gehring et al., 1978; Chen and Blancato, 1989; Reitz et al., 1996) have in common the assumption of a single saturable pathway for the metabolism of VC. However, another published model of VC (Gargas et al., 1990) differed from the models discussed above by the incorporation of a second, linear metabolic pathway (presumed by the authors to be GSH conjugation) in parallel with the saturable (oxidative) pathway. Based on gas uptake studies in the male F344 rat, both a saturable and a linear metabolic component were postulated for VC.

These alternative descriptions of metabolism in the published models of VC were examined in a more in-depth study of VC pharmacokinetics performed for the US Air Force by several of the present authors (Clement International, 1990). The one- and two-pathway descriptions were refit to gas uptake data and then compared with measurements of total metabolism by Gehring et al. (1978) and Watanabe et al. (1976b). Although the two-pathway description provided a significantly better fit to the gas uptake data (adding parameters nearly always improves a fit), the resulting parameters tended to overpredict total metabolism at higher concentrations owing to the presence of the first-order component. In addition, it was not possible to explain the continued increase in glutathione (GSH) depletion measured at the highest exposure levels (where the saturable component was above saturation) because only products of the oxidative metabolism of VC have been shown to react with GSH. In an attempt to provide a better correspondence to the data on both total metabolism and glutathione depletion, two possible refinements to the model were investigated. In the first, direct reaction of VC with GSH was postulated, and in the second, the products of both the saturable and the linear pathways were assumed to react with GSH. Unfortunately, neither description was able to provide a satisfactory correspondence to both total metabolism and GSH depletion data. The analysis suggested that a different formulation featuring two saturable oxidative pathways, both producing reactive metabolites, provided the required behavior.

The PBPK models previously used to conduct a human risk assessment for VC (Chen and Blancato, 1989; Reitz et al., 1996) certainly provide a more biologically plausible basis for estimating human carcinogenic risk than default measures of VC exposure. However, a 2-saturable pathway model structure would have the potential advantage of being able to reproduce experimental data on both total metabolism and GSH depletion, based on a reasonable hypothesis: only saturable oxidative metabolism is involved (no other metabolic pathway for VC has been demonstrated), and only products of oxidative metabolism react with GSH (neither direct reaction nor GST-mediated conjugation of VC with GSH has been demonstrated). This metabolic hy-

pothesis formed the basis for the model development conducted in this study. The model, which will be described in more detail later, is similar to the PBPK model developed by D'Souza and Andersen (1988) to describe vinylidine chloride (VDC) kinetics and toxicity, including the depletion of GSH by the products of VDC metabolism. The chief difference is the use of two saturable pathways instead of one to describe metabolism. The use of a low affinity pathway in parallel with the high affinity pathway is necessary to provide the continued increases in total metabolism and GSH depletion observed with VC in rats.

3. Mechanism of carcinogenicity of VC

Many of the results of the pharmacokinetic and metabolism studies discussed above indicate that like other chlorinated alkenes, VC must be metabolized to cause carcinogenicity (Bartsch and Montesano, 1975). A reactive, short-lived metabolite, which achieves only low steady-state concentrations, is thought to be responsible for the toxic effects of VC (Bolt, 1978). That the toxicity of VC is mediated by the production of reactive metabolites is suggested by the results of in vitro studies in which enhanced mutagenicity was observed if microsomal enzymes of fortified liver homogenates were present (Bartsch et al., 1975; Malaveille et al., 1975; Rannug et al., 1974). The rapid elimination of VC and its major metabolites is also consistent with the theory that a shortly lived, reactive metabolite occurring at concentrations too low for direct observation could be responsible for the carcinogenicity of VC (Bolt et al., 1977).

It has long been a tenet of carcinogenic risk assessment that the mechanism of carcinogenicity for 'genotoxic' carcinogens (sometimes referred to as initiators) involves reaction with DNA, leading to mistranscription during subsequent cell division, causing a loss or change in heritable information which results in a neoplastic daughter cell (Van Duuren, 1988; Singer, 1985). The in vivo formation of four etheno-DNA adducts has been demonstrated following exposure of animals to VC (Laib, 1986; Fedtke et al., 1990; Dosanjh et al., 1994): $1,N^2$-ethenoguanine ($1,N^2$-EG); N^2,3-ethenoguanine (N^2,3-EG); $1,N^6$-etheno-2′-deoxyadenosine (EDA), and $3,N^4$-etheno-2′-deoxycytidine (EDC). These etheno-adducts are highly persistent (Swenberg et al., 1992) and can lead to defective transcription (Singer et al., 1987); for example, EG produces a base pair mismatch ($G->A$ transition) in bacterial assays (Cheng et al., 1991). Single-strand breaks (SSBs) have been detected in liver DNA following inhalation exposure of mice to VC (Walles et al., 1988). (It is generally assumed that SSBs represent an intermediate stage in the excision repair of DNA adducts.) The occurrence of SSBs reached a maximum at exposures of 500 ppm, consistent with saturation of metabolism. It was found that 20% of the SSBs remained after 20 h.

Although there is strong circumstantial evidence linking etheno-DNA adducts with the observed carcinogenicity of VC, there is not yet sufficient information to provide a quantitative link between the tissue concentrations of a specific adduct and the risk of cancer in that tissue. The ratio of the concentrations of the various etheno-adducts in the rat is only marginally consistent across tissues and studies (Fedtke et al., 1990; Swenberg et al., 1992), and there are no data on relative adduct levels in VC-exposed humans. Amount of metabolism would still appear to provide the best dose metric for comparison with tumor incidence.

3.1. Selection of a risk assessment approach

Based on the information described above on the pharmacokinetics, metabolism, and mechanism of carcinogenicity of VC, it is necessary to determine the appropriate approach for conducting a human risk assessment. Clearly, the evidence is strong that the carcinogenicity of VC is related to the production of reactive metabolic intermediates. The most appropriate pharmacokinetic dose metric for a reactive metabolite is the total amount of the metabolite generated divided by the volume of the tissue into which it is produced (Andersen et al., 1987a). In the case of VC, reasonable dose metrics for angiosarcoma would include the total amount of metabolism

divided by the volume of the liver (RISK), or the total amount of metabolism not detoxified by reaction with glutathione, again divided by the volume of the liver (RISKM). A third, less likely possibility, that the GSH conjugate of VC is subsequently metabolized to a reactive species which is responsible for the carcinogenicity, can also be considered by using a dose metric based on the total amount of reaction with GSH divided by the volume of the liver (RISKG). The assumption underlying the use of these dose metrics is that the concentration of the actual carcinogenic moiety, or the extent of the crucial event associated with the cellular transformation, is linearly related to this pseudo-concentration of reactive intermediates, and that the relationship of the actual carcinogenic moiety or crucial event to the dose metric is constant across concentration and species. Specifically, the average amount generated in a single day is used, averaged over the lifetime (i.e. the lifetime average daily dose, or LADD). The use of a dose rate, such as the LADD, rather than total lifetime dose, has been found empirically to provide a better cross-species extrapolation of chemical carcinogenic potency (USEPA, 1992).

Subsequent steps in the carcinogenic mechanism related to specific adduct formation, detection, and repair, as well as to the consequences of DNA mistranscription and the potential impact of increased cell proliferation, have only been sketchily outlined and have not yet reached the point where they could be incorporated into a risk assessment in any quantitative form. However, there appears to be sufficient evidence to justify the assumption that VC acts as a classic initiator, producing genetic transformations through direct reaction of its metabolites with DNA. Therefore, the traditional assumption of low-dose linearity of risk appears to be warranted, and the linearized multistage (LMS) model would seem to be the most appropriate for low-dose extrapolation.

4. Description of PBPK model for VC

The PBPK model for VC developed in this study is shown in Fig. 2. As mentioned earlier, the model is basically an adaptation of a previously developed PBPK model for vinylidene chloride (D'Souza and Andersen, 1988). For a poorly soluble, volatile chemical like VC, only four tissue compartments are required: a richly perfused tissue compartment which includes all of the organs except the liver; a slowly perfused tissue compartment which includes all of the muscle and skin tissue; a fat compartment which includes all of the fatty tissues; and a liver compartment. All metabolism is assumed to occur in the liver, which is a good assumption in terms of the overall kinetics of VC, but which would have to be revised to include target-tissue-specific metabolism if a serious attempt were to be made to perform a VC risk assessment for a tissue other than the liver (Andersen et al., 1987a). The model also assumes flow-limited kinetics, or venous equilibration; that is, that the transport of VC between blood and tissues is fast enough for steady state to be reached within the time it is transported through the tissues in the blood.

Metabolism of VC is modeled by two saturable pathways, one high affinity, low capacity (with parameters VMAX1C and KM1) and one low affinity, high capacity (with parameters VMAX2C and KM2). Subsequent metabolism is based on the metabolic scheme shown in Fig. 1: the reactive metabolites (whether CEO, CAA, or other intermediates) may then either be metabolized further, leading to CO_2, react with GSH, or react with other cellular materials, including DNA. Because exposure to VC has been shown to deplete circulating levels of GSH, a simple description of GSH kinetics was also included in the model.

The parameters for the model are listed in Tables 1 and 2. The physiological parameters are EPA reference values (USEPA, 1988), except for the alveolar ventilation (QPC) in the human, which was calculated from the standard EPA value for the ventilation rate in the human, 20 m^3 day^{-1}, assuming a 33% pulmonary dead-space (USEPA, 1988). The value for the cardiac output (QCC) in the human was selected to correspond to the same workload as the standard EPA ventilation using data from Astrand and Rodahl (1970). For modeling of the closed chamber studies with

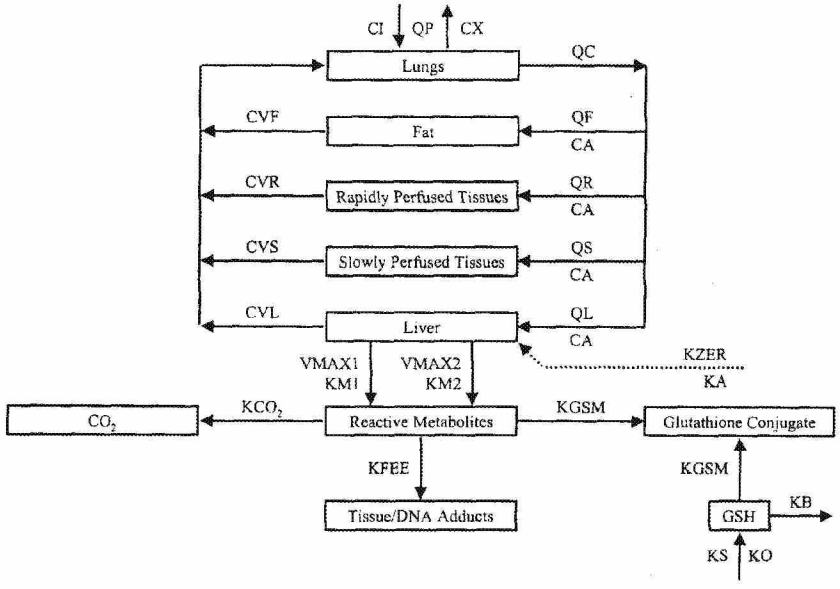

Fig. 2. Diagram of the PBPK model of VC. Abbreviations: QP, alveolar ventilation; CI, inhaled concentration; CX, exhaled concentration; QC, cardiac output; QF, CVF-blood flow to, and venous concentration leaving, the fat; QR, CVR, blood flow to, and venous concentration leaving, the richly perfused tissues (most organs); QS, CVS, blood flow to, and venous concentration leaving, the slowly perfused tissues (e.g. muscle); QL, CVL, blood flow to, and venous concentration leaving, the liver; VMAX1,KM1, capacity and affinity for the high affinity oxidative pathway enzyme (CYP 2E1); VMAX2,KM2, capacity and affinity for the lower affinity oxidative pathway enzymes, (e.g. CYP 2C11/6); KZER, zero-order rate constant for uptake of VC from drinking water; KA, first-order rate constant for uptake of VC from corn oil; KCO2, first-order rate constant for metabolism of VC to CO_2; KGSM, first-order rate constant for reaction of VC metabolites with GSH; KFEE, first-order rate constant for reaction of VC metabolites with other cellular materials, including DNA; KB, first-order rate constant for normal turnover of GSH; KO, zero-order rate constant for maximum production of GSH; KS-parameter controlling rate of recovery of GSH from depletion.

human subjects, more typical resting values of 15 for cardiac output (QCC) and 18 for alveolar ventilation (QPC) were used. In some cases, it was also necessary to slightly vary the alveolar ventilation and cardiac output of the animals in the closed chamber studies in order to obtain acceptable simulations of those experiments. The partition coefficients for Fisher-344 (F344) rats were taken from Gargas et al. (1989), and those for Sprague–Dawley rats were taken from Barton et al. (1995). The Sprague–Dawley values were also used for modeling of Wistar rats. Blood/air partition coefficients for the other species were obtained from Gargas et al. (1989), and the corresponding tissue/blood partition coefficients were estimated by dividing the Sprague–Dawley rat tissue/air partition coefficients by the appropriate blood/air value.

The affinity for the 2E1 pathway (KM1) in the rat, mouse, and hamster was set to 0.1 on the basis of studies of the competitive interactions between CYP2E1 substrates in the rat (Barton et al., 1995; Andersen et al., 1987b). The affinity used for the non-2E1 pathway (KM2) in the mouse and rat was set during the iterative fitting of the rat total metabolism, glutathione depletion, and rate of metabolism data, described below. The capacity parameters for the two oxidative pathways (VMAX1C and VMAX2C) in the mouse, rat, and hamster were estimated by fitting the model to data from closed-chamber exposures with each of the species and strains of interest

(Barton et al., 1995; Bolt et al., 1977; Clement International, 1990; Gargas et al., 1990), holding all of the other model parameters fixed and requiring a single pair of values for VMAX1C and VMAX2C to be used for all of the data on a given sex/strain/species. Figs. 3 and 4 show examples of the results of this fitting process for the male B6C3F1 mouse and male Wistar rat, respectively.

Initial estimates for the subsequent metabolism of the reactive metabolites and for the glutathione submodel in the rat were taken from the model for vinylidene chloride (D'Souza and Andersen, 1988). These parameter estimates, along with the estimates for VMAX2C and KM2, were then refined for the case of VC in the Sprague–Dawley rat using an iterative fitting process which included the closed chamber data for the Sprague–Dawley and Wistar rat (Barton et al., 1995; Bolt et al., 1977; Clement International, 1990) along with data on glutathione depletion (Jedrychowski et al., 1985; Watanabe et al.,

Table 1
Model parameters and dose metrics for the vinyl chloride model

		Mouse (CV-%)[a]	Rat (CV-%)	Human (CV-%)
BW	Body weight (kg)	– [b](11)	– (11)	70.0 (30)
QPC	Alveolar ventilation ($l\ h^{-1}$, 1 kg animal[c])	30.0 (58)	21.0 (58)	24.0 (16)
QCC	Cardiac output ($l\ h^{-1}$, 1 kg animal[c])	18.0 (9)	18.0 (9)	16.5 (9)
Tissue blood flows (fraction of cardiac output)				
QRC	Flow to rapidly perfused tissues	0.51 (50)	0.51 (50)	0.5 (20)
QFC	Flow to fat	0.09 (60)	0.09 (60)	0.05 (30)
QSC	Flow to slowly perfused tissues	0.15 (40)	0.15 (40)	0.19 (15)
QLC	Flow to liver	0.25 (96)	0.25 (96)	0.26 (35)
Tissue volumes (fraction of body weight)				
VSC	Volume of slowly perfused tissues	0.77 (30)	0.75 (30)	0.63 (30)
VFC	Volume of fat	– (30)	– (30)	0.19 (30)
VRC	Volume of richly perfused tissues	0.035 (30)	0.05 (30)	0.064 (10)
VLC	Volume of liver	0.055 (6)	0.04 (6)	0.026 (5)
Partition coefficients				
PB	Blood/air	2.26 (15)	2.4 (15)	1.16 (10)
PF	Fat/blood	10.62 (30)	10.0 (30)	20.7 (30)
PS	Slowly perfused tissue/blood	0.42 (20)	0.4 (20)	0.83 (20)
PR	Richly perfused tissue/blood	0.74 (20)	0.7 (20)	1.45 (20)
PL	Liver/blood	0.74 (20)	0.7 (20)	1.45 (20)
Model parameters and dose metrics for the vinyl chloride model Metabolic parameters				
VMAX1C	Maximum velocity of first saturable pathway ($mg\ h^{-1}$, 1 kg animal[c])	– (20)	– (20)	4.0 (30)
KM1	Affinity of first saturable pathway ($mg\ l^{-1}$)	0.1 (30)	0.1 (30)	1.0 (50)
VMAX2C	Maximum velocity of second saturable pathway ($mg\ h^{-1}$, 1 kg animal[c])	– (20)	– (20)	0.1 (0)
KM2	Affinity of second saturable pathway ($mg\ l^{-1}$)	10.0 (30)	10.0 (30)	10.0 (50)

Table 1 (*Continued*)

		Mouse (CV-%)[a]	Rat (CV-%)	Human (CV-%)
GSH parameters				
KCO2C	First order CEO breakdown to CO_2	1.6 (20)	1.6 (20)	1.6 (20)
KGSMC	Conjugated rate constant with metabolite	0.13 (20)	0.13 (20)	0.13 (20)
KFEEC	Conjugated rate constant with non-GSH	35.0 (20)	35.0 (20)	35.0 (20)
GSO	Initial GSH concentration	5800.0 (20)	5800.0 (20)	5800.0 (20)
KBC	First order rate constant for GSH breakdown	0.12 (20)	0.12 (20)	0.12 (20)
KS	Constant controlling resynthesis	2000.0 (20)	2000.0 (20)	2000.0 (20)
KOC	Zero order production of GSH	28.5 (20)	28.5 (20)	28.5 (20)
Dosing parameters				
KA	Oral uptake rate (h)	3.0 (50)	3.0 (50)	3.0 (50)

[a]CV-%, coefficient of variation = 100 × S.D./mean.
[b]See Table 2.
[c]Scaled by body weight raised to the 3/4 power.

1976c), total metabolism (Gehring et al., 1978), and CO_2 elimination (Watanabe and Gehring, 1976). Since this last data set was obtained for oral dosing with VC in corn oil, a value for KA, the oral uptake rate from corn oil, was estimated from fitting of separate data on blood concentrations following dosing of rats with VC in corn oil (Withey, 1976). The results of this iterative process are illustrated in Figs. 4–8, and the resulting parameters are listed in Tables 1 and 2. The parameters obtained for the rat were used for the other species with appropriate allometric scaling (e.g. body weight to the $-1/4$ for the first order rate constants).

Parameterization of the P450 metabolism pathways in the human was accomplished as follows. There is no evidence of high capacity, low affinity P450 metabolism for chlorinated ethylenes in the human based on the results of occupational kinetic studies for another chemical, TCE, therefore, VMAX2C in the human was set to zero. The ratio of VMAX1C to KM1 could be estimated by

Table 2
Strain/study-specific parameter values

		BW	VFC	VMAX1C	VMAX2C
Swiss albino mice (inhalation study)	Male	0.044	0.13	8.0	0.1[a]
	Female	0.040	0.12	5.0	3.0
Sprague–Dawley rats (inhalation study)	Male – low dose	0.638	0.19	4.0	2.0
	Male – high dose	0.433	0.13	4.0	2.0
	Female – low dose	0.485	0.20	3.0	0.1[a]
	Female – high dose	0.321	0.14	3.0	0.1[a]
Sprague–Dawley rats (gavage study)	Male – low dose	0.632	0.19	4.0	2.0
	Male – high dose	0.405	0.12	4.0	2.0
	Female – low dose	0.445	0.18	3.0	0.1[a]
	Female – high dose	0.301	0.13	3.0	0.1[a]
Wistar rats (dietary study)	Male	0.436	0.14	4.0	2.0
	Female	0.245	0.11	3.0	0.1[a]

[a]The value of this parameter was normally set to zero. It was only set to 0.1 for the PBPK_SIM runs. The variance for this parameter was set to zero in the PBPK_SIM runs.

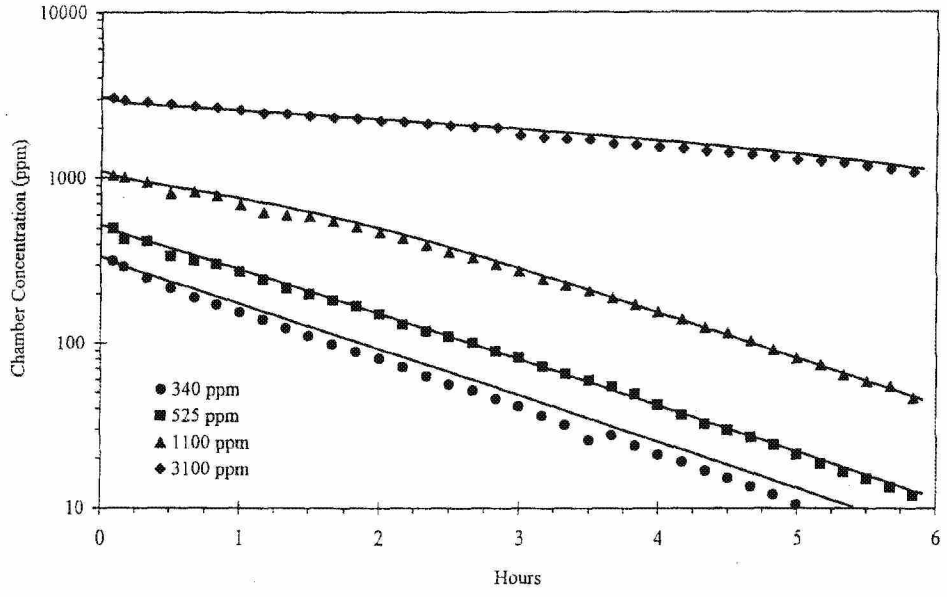

Fig. 3. Model predictions (lines) and experimental data (symbols) for the chamber concentration during exposure of male B6C3F1 mice to VC in a closed, recirculated chamber (data taken from Clement International, 1990).

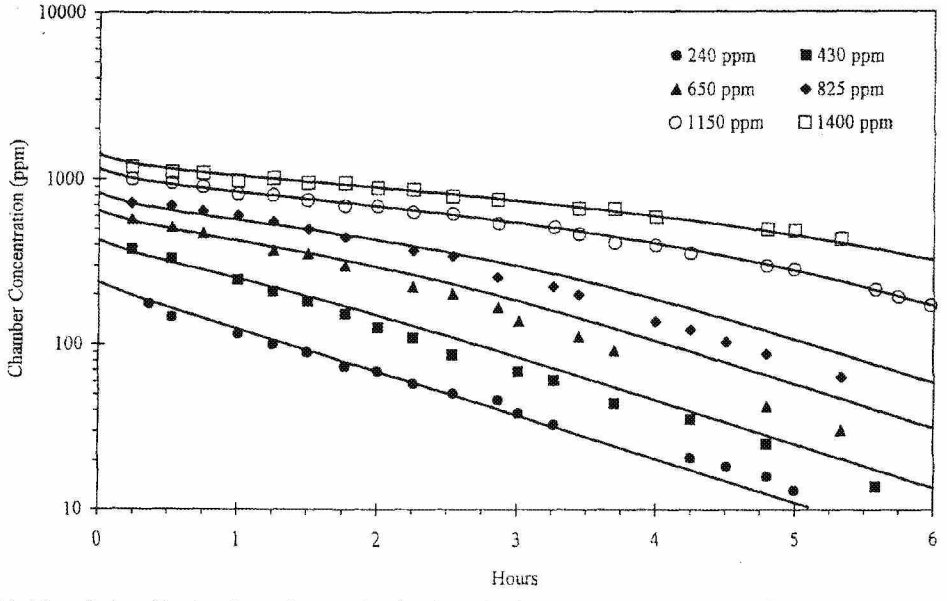

Fig. 4. Model predictions (lines) and experimental data (symbols) for the chamber concentration during exposure of male Wistar rats to VC in a closed, recirculated chamber (data taken from Bolt et al., 1977).

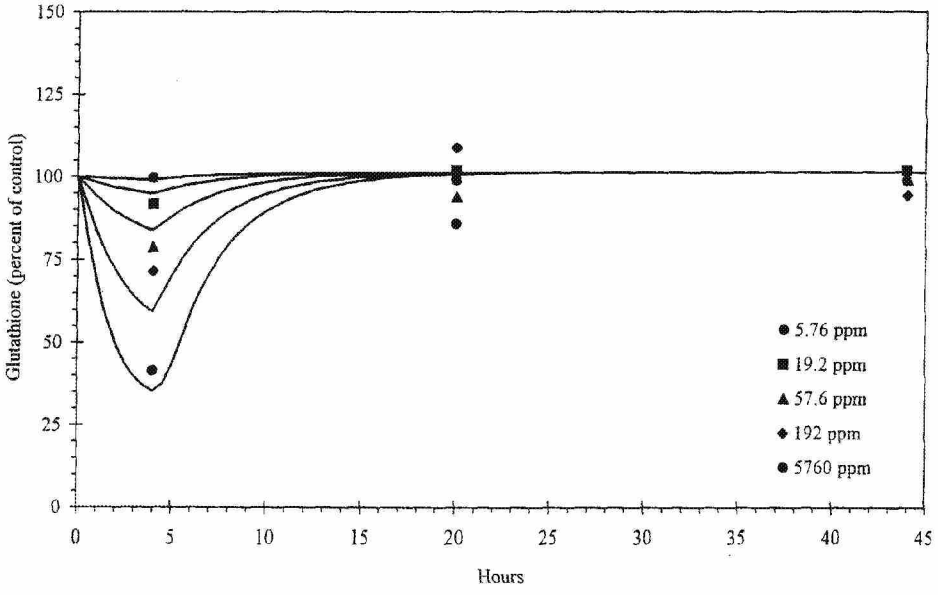

Fig. 5. Model-predicted (lines) and experimentally-determined (symbols) glutathione concentrations (as percent of control animal levels) 0, 20, and 44 h following 4-h inhalation exposures to VC at concentrations of (top to bottom) 15, 50, 150, 500 and 15000 mg/m^3 (data taken from Jedrychowski et al., 1985).

fitting the model to data from closed chamber studies with two human subjects (Buchter et al., 1978), in a manner entirely analogous to the method used for the animal closed chamber analysis. The result of fitting the data on one of the two subjects is shown by the upper curve in Fig. 9a, and the model prediction using the value estimated from this subject is compared with the data from the second subject in Fig. 9b. The precision of the estimate of VMAX1C/KM1 can be evaluated by a comparison of the two model runs shown in these figures, for KM1 = 1.0 and 0.1. It can be seen that the ratio of VMAX1C/KM1 varies between the two subjects. This variability of CYP2E1 activity in the human is not surprising; several studies have demonstrated a variability of human CYP2E1 activity of roughly an order of magnitude (Reitz et al., 1989; Sabadie et al., 1980). Much lower variability is observed in the inbred strains typically used in animal studies; for example, the coefficient of variation (standard deviation divided by the mean) for CYP2E1 activity in rats in one study of rodents was only 14% (Sabadie et al., 1980). The wide variability in human CYP2E1 activity is an important consideration for estimating the potential difference between average population risk and individual risk in a human cancer risk assessment for materials like VC, whose carcinogenicity depends on metabolic activation. The significance of this variability was further evaluated using a Monte Carlo analysis, which is discussed later in this report, and is illustrated in Figs. 9 and 10.

In order to obtain separate estimates of VMAX1C and KM1 in the human, a higher exposure concentration closer to metabolic saturation would be required. Fortunately, cross-species scaling of CYP2E1 between rodents and humans appears to follow allometric expectations for metabolism very closely, i.e. the metabolic capacity scales approximately according to body weight raised to the 3/4 power (Andersen et al., 1987a). Support for the application of this principal to VC can be obtained from data on the metabolism

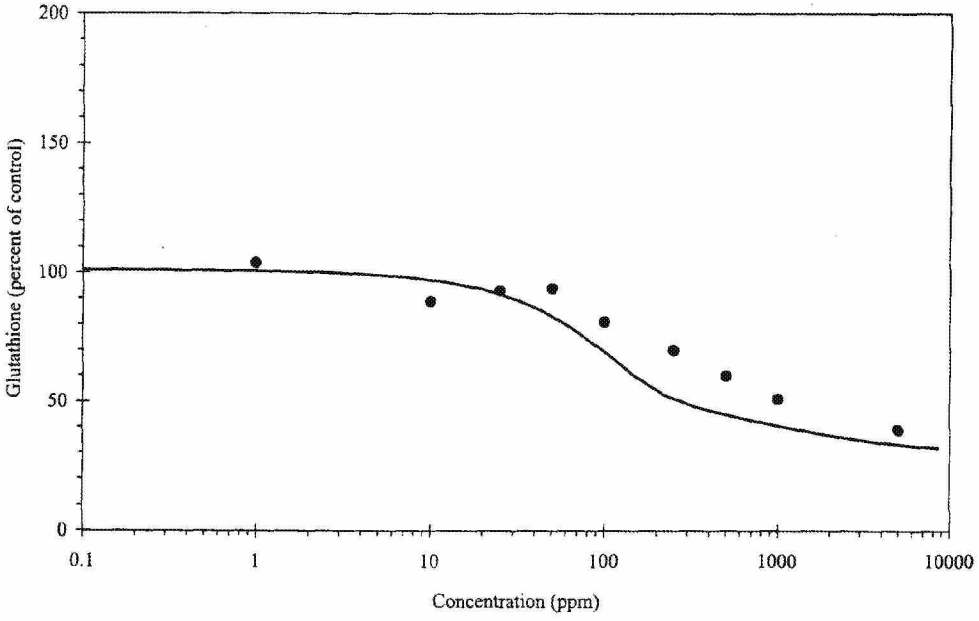

Fig. 6. Model-predicted (lines) and experimentally-determined (symbols) glutathione concentrations (as percent of control animal levels) immediately following 6-h inhalation exposures to VC (data taken from Watanabe et al., 1976c).

of VC in non-human primates (Buchter et al., 1980). Based on data for the dose-dependent metabolic elimination of VC in the rhesus monkey, the maximum capacity for metabolism can be estimated to be approximately 50 μmol h^{-1} kg^{-1}. This equates to a VMAX1C (the allometrically scaled constant used in the model) of approximately 4 mg h^{-1} for a 1-kg animal, a value which is in the same range as those estimated for the rodents from the closed chamber exposure data. The similarity of VMAX1C in humans and rats is also supported by an in vitro study, which found the activity of human microsomes to be 84% of the activity of rat microsomes. Based on these comparisons, the human VMAX1C was set to the primate value and KM1 was calculated using this value of VMAX1C and the ratio of VMAX1C/KM1 obtained from the closed chamber analysis. The ability of the resulting human model to reproduce constant concentration inhalation exposure data (Buchter et al., 1978) is shown in Fig. 10a,b. From a comparison of the model predictions for KM1 = 1.0 and 0.1, it can be seen that the reproduction of parent chemical concentrations in a constant concentration inhalation exposure is not a particularly useful test of the accuracy of the metabolism parameters in a PBPK model of a volatile compound. Based on the results of the Monte Carlo Analysis, the discrepancies or agreement between the model and the data are primarily due to details of the physiological description of the individual, such as fat content, ventilation rate, blood/air partition, etc., rather than rate of metabolism.

5. Comparison of risk estimates for human VC inhalation

The model just described was used to calculate each of the pharmacokinetic dose metrics for angiosarcoma (RISK, RISKM, and RISKG) in the most informative of the animal bioassays (Maltoni et al., 1981, 1984; Maltoni and Cotti, 1988; Feron

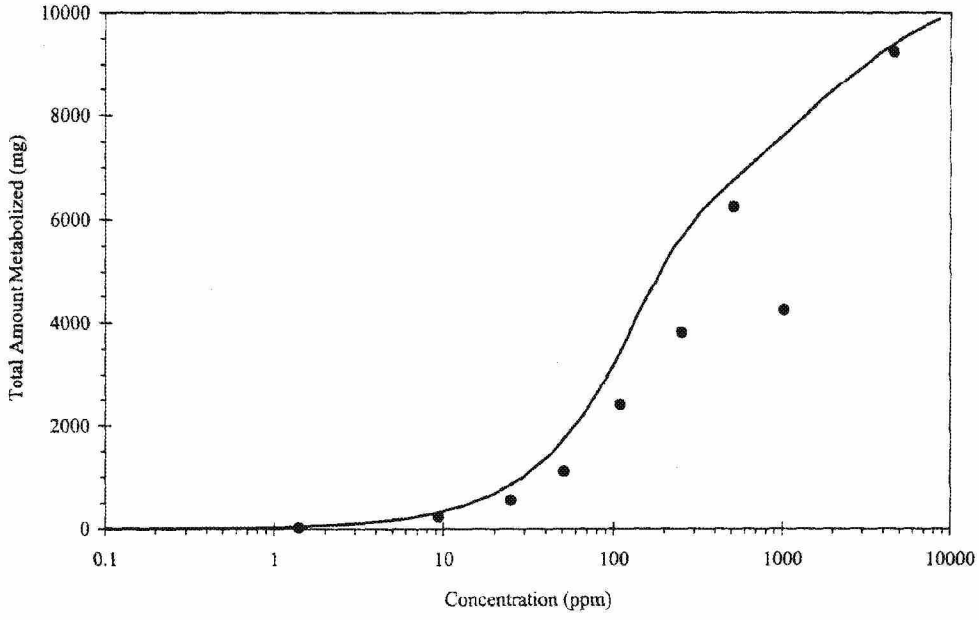

Fig. 7. Model-predicted (lines) and experimentally-determined (symbols) total amount metabolized during 6-h inhalation exposures to VC (data taken from Gehring et al., 1978).

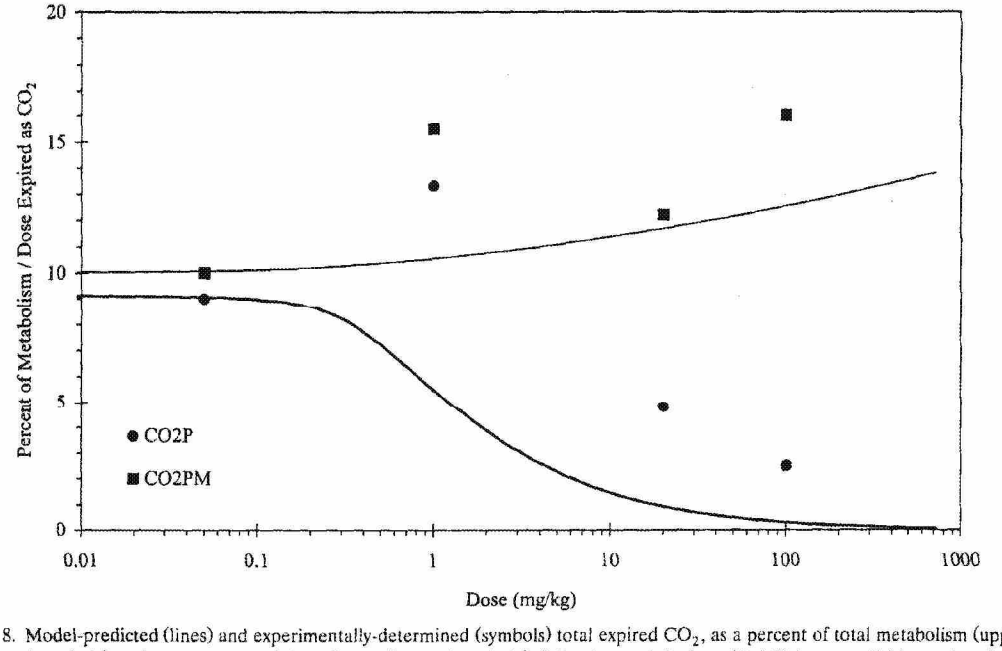

Fig. 8. Model-predicted (lines) and experimentally-determined (symbols) total expired CO_2, as a percent of total metabolism (upper line and symbols) and as a percent of dose (lower line and symbols), following oral dosing with VC in corn oil (data taken from Watanabe and Gehring, 1976).

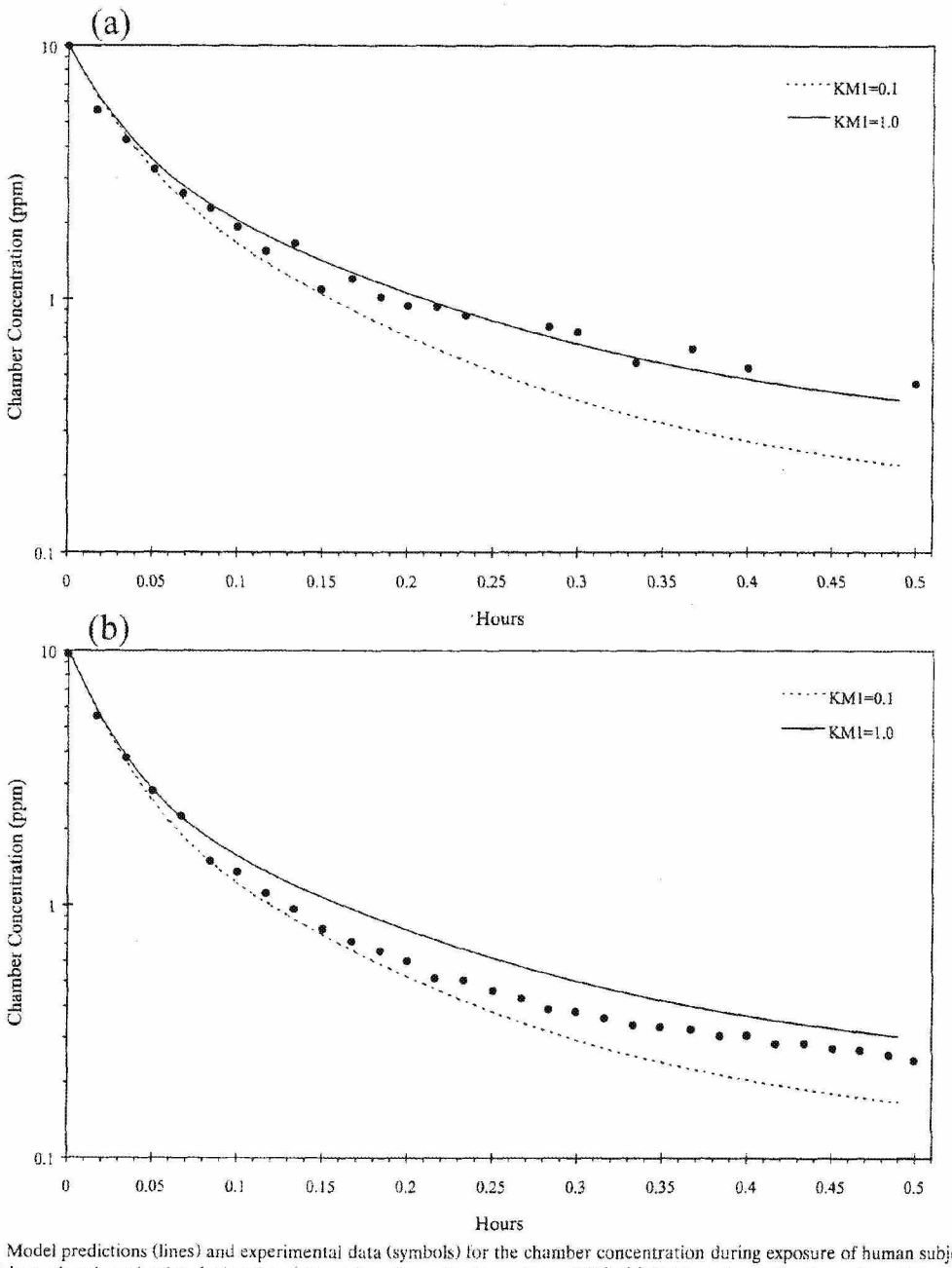

Fig. 9. Model predictions (lines) and experimental data (symbols) for the chamber concentration during exposure of human subjects to VC in a closed, recirculated chamber (data taken from Buchter et al., 1978). (a) Subject A — the lines show the model predictions for (top to bottom) KM1 = 1.0 and 0.1; (b) Subject B — the lines show the model predictions for (top to bottom) KM1 = 1.0 and 0.1. The rest of the model parameters are those shown for the human in Tables 3 and 4.

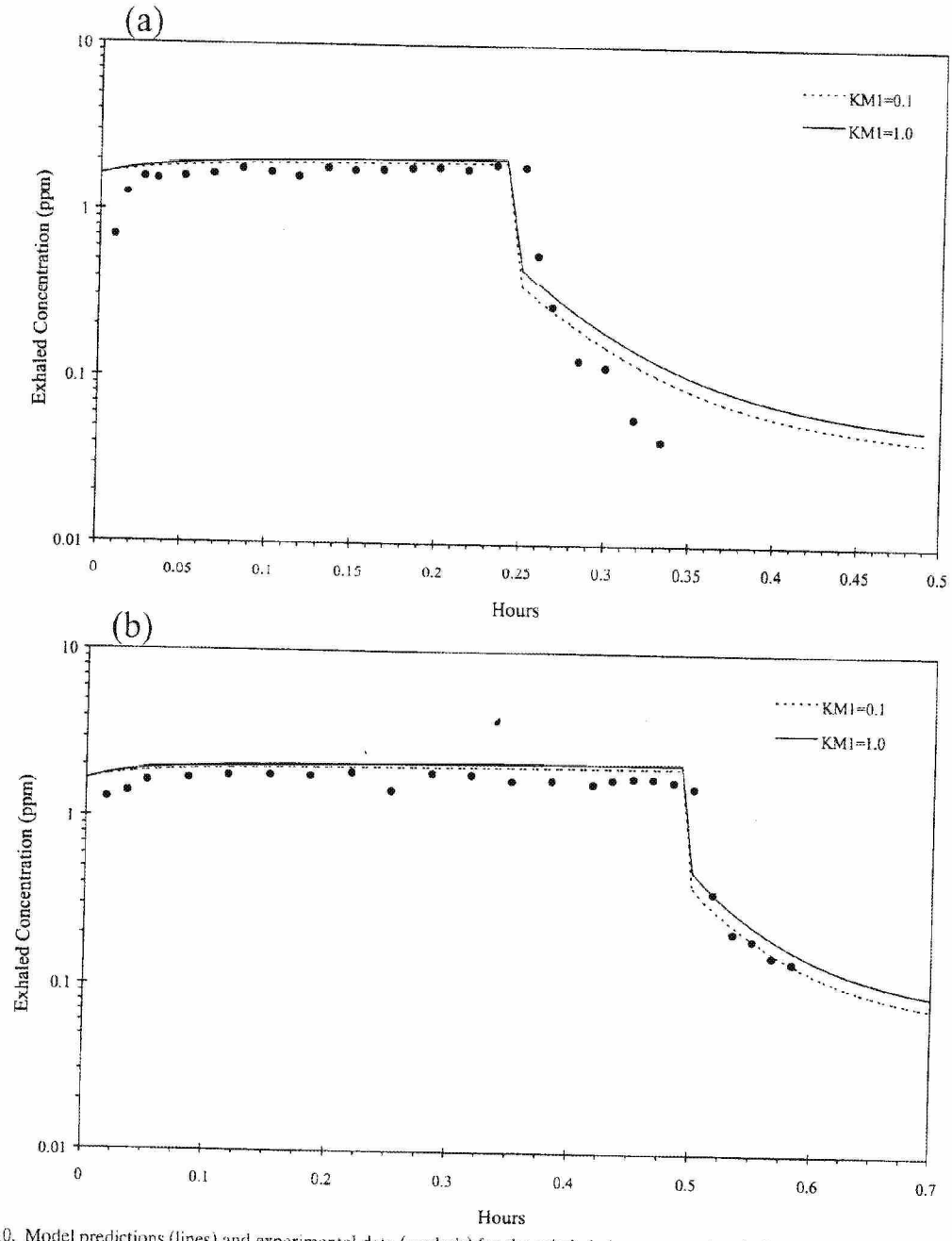

Fig. 10. Model predictions (lines) and experimental data (symbols) for the exhaled air concentration during and following inhalation exposure of human subjects to a constant concentration of 2.5 ppm VC (data taken from Buchter et al., 1978). (a) Subject A — the lines show the model predictions for (top to bottom) KM1 = 1.0 and 0.1; (b) Subject B — the lines show the model predictions for (top to bottom) KM1 = 1.0 and 0.1. The rest of the model parameters are those shown for the human in Tables 3 and 4.

et al., 1981), as well as for human inhalation exposure. The results of these calculations for the RISK dose metric (milligrams metabolized per litre of liver assuming the density of the liver is 1 kg l^{-1}) are shown in Table 3. The 95% upper confidence limits (UCLs) on the human risk estimates for lifetime exposure to 1 ppm VC were then calculated on the basis of each of the sets of animal bioassay data, using the LMS model. As shown in Table 4, the resulting risk estimates for lifetime human exposure to 1 ppm VC, based on the RISK dose metric, range from 1.52×10^{-3} to 15.7×10^{-3}. Because saturation of metabolism occurs well above the 1 ppm concentration in the human, estimates of risk below 1 ppm can be adequately estimated by assuming linearity (e.g. the risk estimates for lifetime human exposure to 1 ppb of VC would range from approximately

Table 3
Dose metric values for angiosarcomas

Study	Species	Duration	Dose	Incidence	Daily dose metric RISK (mg l^{-1})	Lifetime average daily dose RISK (mg l^{-1})
Inhalation	Human	Continuous	1 ppm		1.614	1.614
Drinking water		exposure	0.0286 mg kg^{-1} day^{-1}		0.603	0.603
Maltoni and Cotti (1988)	Swiss	4 h day^{-1}, 5	0 ppm	0/80		
(BT4)	albino	days $week^{-1}$	50 ppm	1/30	161.924	33.363
Inhalation	mice (M)	for 30 of 104	250 ppm	9/30	775.615	159.811
		weeks	500 ppm	6/30	1245.220	256.570
			2500 ppm	6/29	1434.800	295.632
			6000 ppm	2/30	1479.270	304.795
			10000 ppm	1/26	1505.580	310.216
	Swiss	4 h day^{-1}, 5	0 ppm	0/70		
	albino	days $week^{-1}$	50 ppm	0/30	156.907	32.330
	mice (F)	for 30 of 104	250 ppm	9/30	673.015	138.671
		weeks	500 ppm	8/30	887.253	182.813
			2500 ppm	10/30	1197.670	246.773
			6000 ppm	11/30	1341.160	276.338
			10000 ppm	9/30	1405.330	289.560
Maltoni et al. (1981, 1984)	Sprague–	4 h day^{-1}, 5	0 ppm	0/73		
(BT15 and BT1)	Dawley	days $week^{-1}$	1 ppm	0/55	2.398	0.606
Inhalation	rats (M)	for 52 of 147	5 ppm	0/47	11.985	3.028
		weeks	10 ppm	1/46	23.933	6.047
			25 ppm	4/40	59.552	15.047
		4 h day^{-1}, 5	50 ppm	1/29	117.989	32.463
		days $week^{-1}$	250 ppm	2/26	473.425	130.254
		for 52 of 135	500 ppm	6/28	593.928	163.409
		weeks	2500 ppm	7/24	803.198	220.986
			6000 ppm	10/25	911.248	250.714
	Sprague–	4 h day^{-1}, 5	0 ppm	0/45		
	Dawley	days $week^{-1}$	1 ppm	0/48	2.343	0.592
	rats (F)	for 52 of 147	5 ppm	0/43	11.698	2.956
		weeks	10 ppm	0/42	23.332	5.895
			25 ppm	1/41	57.838	14.614
		4 h day^{-1},	50 ppm	0/26	113.653	31.270
		5 days $week^{-1}$	250 ppm	1/28	375.989	103.447
		for 52 of 135	500 ppm	0/22	425.029	116.939
		weeks	2500 ppm	6/26	488.374	134.367
			6000 ppm	3/17	522.359	143.718

Table 3 (*Continued*)

Study	Species	Duration	Dose	Incidence	Daily dose metric RISK ($mg\ l^{-1}$)	Lifetime average daily dose RISK ($mg\ l^{-1}$)
Maltoni et al. (1981, 1984) (BT11) Gavage	Sprague–Dawley rats (M)	5 days $week^{-1}$ for 52 of 136 weeks	0 mg kg^{-1} day^{-1}	0/60		
			0.021 mg kg^{-1} day^{-1}	0/15	0.488	0.133
			0.214 mg kg^{-1} day^{-1}	0/15	4.962	1.355
			0.714 mg kg^{-1} day^{-1}	1/21	16.373	4.472
			2.38 mg kg^{-1} day^{-1}	0/34	50.390	13.762
			11.9 mg kg^{-1} day^{-1}	4/39	133.231	36.387
			35.7 mg kg^{-1} day^{-1}	8/36	203.079	55.463
	Sprague–Dawley rats (F)		0 mg kg^{-1} day^{-1}	0/73		
			0.021 mg kg^{-1} day^{-1}	0/18	0.477	0.130
			0.214 mg kg^{-1} day^{-1}	1/19	4.835	1.321
			0.714 mg kg^{-1} day^{-1}	2/29	15.800	4.315
			2.38 mg kg^{-1} day^{-1}	0/37	45.330	12.380
			11.9 mg kg^{-1} day^{-1}	6/34	102.763	28.066
			35.7 mg kg^{-1} day^{-1}	9/35	143.866	39.291
Feron et al. (1981) Diet	Wistar rats (M)	135 weeks 7 days $week^{-1}$	0 mg kg^{-1} day^{-1}	0/55		
			1.7 mg kg^{-1} day^{-1}	0/58	39.539	39.539
			5.0 mg kg^{-1} day^{-1}	6/56	116.103	116.103
			14.1 mg kg^{-1} day^{-1}	27/59	325.845	325.845
	Wistar rats (F)	144 weeks 7 days $week^{-1}$	0 mg kg^{-1} day^{-1}	0/57		
			1.7 mg kg^{-1} day^{-1}	0/58	38.611	38.611
			5.0 mg kg^{-1} day	2/59	113.243	113.243
			14.1 mg kg^{-1} day^{-1}	9/57	316.628	316.628

1.52×10^{-6} to 15.7×10^{-6}). It should be noted that although the animal studies represent both inhalation and oral exposure, the risk predictions in each case are for human inhalation exposure.

Only the results for the RISK dose metric (milligrams metabolized per kilogram of liver) are shown in Tables 3 and 4. The *P*-values for goodness of fit of the 1-stage model using the other alternative dose metrics (RISKM, and RISKG) were very similar; therefore, it is not possible to select one metric over another on the basis of agreement with the dose–response of the incidence data. Fortunately, the risks predicted for each of the studies by the various dose metrics were roughly similar. The RISKM metric, which is the most biologically plausible, resulted in lower risks than the RISK metric (ranging from 0.50×10^{-3} to 12.46×10^{-3} ppm); while the RISKG metric, which is probably the least likely, resulted in risk estimates up to 30% higher than those shown in Table 4.

There are no consistent differences between risk estimates based on male and female animals, with the female-based risks being higher than the

Table 4
Human risk estimates based on angiosarcoma incidence

95% UCL risk/1000/ppm	Risk
Maltoni and Cotti (1988) BT4 – Inhalation	
Male mice	1.52
Female mice	3.27
Maltoni et al. (1981, 1984) BT14/BT1 – Inhalation	
Male rats	5.17
Female rats	2.24
Maltoni et al. (1981, 1984) BT11 – Gavage	
Male rats	8.68
Female rats	15.70
Feron et al. (1981) – Diet	
Male rats	3.05
Female rats	1.10

male-based risks in some studies, and lower in others, but generally agreeing within a factor of two to three. The risk estimates based on inhalation studies with mice (0.5×10^{-3} to 4.3×10^{-3} ppm) agree very well with those based on inhalation studies with rats (1.46×10^{-3} to 5.94×0^{-3} ppm), demonstrating the ability of pharmacokinetics to integrate dose–response information across species.

The risks estimated from the dietary administration of VC (0.94×10^{-3} to 3.13×10^{-3} ppm) are also in good agreement with those obtained from the inhalation bioassays, showing good route-to-route correspondence of potency based on the pharmacokinetic dose metric. However, the estimates based on oral gavage of VC in vegetable oil (6.58×10^{-3} to 16.3×10^{-3} ppm) are approximately sixfold higher than either dietary or inhalation exposure. It has previously been noted in studies with chloroform that administration of the chemical in corn oil results in more marked hepatotoxic effects than observed when the same chemical is provided in an aqueous suspension (Bull et al., 1986). It has also been demonstrated that administration of corn oil alone leads to an increase in peroxisomal oxidative enzyme activity in rats (DeAngelo et al., 1989). The toxicity and oxidative environment created in the liver by continual dosing with large volumes of vegetable oil could serve to potentiate the effects of genotoxic carcinogens in the liver. In support of this suggestion, Newberne et al. (1979) found that incorporation of corn oil into the diet increased the yield of aflatoxin B_1-induced tumors in rats. A similar phenomenon could be responsible for the apparently higher potency of VC when administered by oil gavage compared to incorporation in the diet.

5.1. Epidemiological analysis of vinyl chloride carcinogenicity

In order to evaluate the plausibility of the risks predicted on the basis of the animal data, risk calculations were also performed on the basis of available epidemiological data. A linear relative risk dose–response model was used for analysis of the human data:

$$O = E(1 + \alpha * d)$$

where O is the observed number of liver tumors, E is the expected number of such tumors apart from any exposure, d is a cumulative dose metric (see Section 7) and α is a potency parameter that can be estimated by maximum likelihood techniques. Then it follows that the lifetime probability of liver cancer, $P(d)$, can be estimated by:

$$P(d) = P_0(1 + \alpha * d)$$

where P_0 is the background probability of liver cancer death estimated using the US Cancer Mortality Rates and Trends (NCI, 1983). Actually, the lifetime risk should be estimated by a lifetable method, but the above approximation should be close enough for the purpose of these comparative potency estimates.

Now suppose that for a particular exposure scenario (e.g. a VC atmospheric concentration of 50 ppm, 8 h a day, 5 days per week), the PBPK model predicts an average daily internal dose metric of X. Then the cumulative exposure that should be used in the dose–response model is $X \times Y$, where Y is the number of years of such exposure. Note that to compute this PBPK-based cumulative dose, we must have an estimate of the 'typical' workplace exposure concentration for each subcohort, separate from the number of years of exposure for the subcohort, rather than just a cumulative dose estimate. Only after the internal dose has been calculated with the PBPK model can the duration of exposure be applied to get a cumulative internal dose.

To obtain pharmacokinetic, human-based risk estimates, the PBPK model was run for the exposure scenario appropriate to each of the selected subcohorts from the studies discussed below. The resulting internal dose metrics were multiplied by the appropriate durations to obtain the cumulative internal doses (amount metabolized per volume of liver), which were then input into the relative risk model along with the observed and

expected liver cancer deaths for each subcohort to get an estimate of the maximum likelihood estimate and 95% confidence interval for α. Then, to determine the risk associated with a continuous lifetime exposure to 1 ppm for comparison with the animal results, the PBPK model was run for a 1 ppm continuous exposure, and the average daily value of the various internal dose metrics was calculated. Multiplying the dose metrics by 70 years gives the appropriate cumulative dose for the relative risk model. For a sufficiently small P_0 (which it should be for liver cancer in humans), the extra risk for a lifetime exposure to 1 ppm VC will be approximately:

$$P_0 * \alpha * d_1$$

where d_1 is the cumulative internal dose for 1 ppm continuous exposure. Using the 95% upper bound on the estimate for α provides a 95% upper confidence limit on the lifetime risk per ppm for comparison with the animal-based results obtained with the LMS model.

Three epidemiological studies that associated increased liver cancer with exposure to VC, and that provide sufficient information to support separate exposure concentration and duration estimates (as opposed to just cumulative exposure estimates), were selected for this study: Fox and Collier (1977), Jones et al. (1988) and Simonato et al. (1991).

5.1.1. Fox and Collier (1977)

This study is probably the best with respect to providing information about duration of employment for different exposure-level groupings (see their Table 2). We have previously estimated the average exposure levels to be 12.5, 70 and 300 ppm for the low, medium and high exposure groups, respectively (Clement Associates, 1987); for comparison Chen and Blancato (1989) estimated averages of 11, 71 and 316 ppm. For the constant exposure groups, these concentrations were input into the human PBPK model, assuming 8 h day^{-1} and 5 days week^{-1} exposure, to get average daily internal dose metrics, which were then multiplied by the duration averages (assumed to be 5, 15 and 27 years) to get cumulative doses. For the intermittent exposure groups, exposure for 2 h day^{-1}, 5 days week^{-1} was assumed.

A weighted average was then performed of the cumulative doses within each exposure group (high, medium, and low), across duration of exposure categories and constant vs. intermittent groups. This must be done because observed and expected numbers of liver cancers are reported only by exposure group (see their Table 9). The weighting was performed using the number of workers in the various subcohorts (their Table 2).

The resulting weighted dose estimates for each internal dose metric were then input into the relative risk model along with the observed and expected tumors:

Cumulative dose	Obs.	Exp.
Average low cumulative dose	1	0.75
Average medium cum. dose	1	0.77
Average high cum dose	2	0.13

The resulting risk estimates are shown in Table 5. The range of risk estimates reflects uncertainty in the appropriate value for P_0, the background probability of death from liver cancer. The lower risk estimate was calculated using the value of P_0 derived in the Fox and Collier study, while the higher risk estimate was calculated using an estimate of the lifetime liver cancer mortality rate in the US population (Chen and Blancato, 1989). An important factor to be aware of in interpreting these results is that the classification into exposure groups in this study was based on the maximum exposure level that a worker experienced. This leads to overestimation of cumulative exposure, particularly for the workers in the medium and high groups and, therefore, a probable underestimation of risk when using the linear relative risk model.

Table 5
Human-based risk estimates

95% UCL risk/1000/ppm	
Fox and Collier (1977)	0.71–4.22
Jones et al. (1988)	0.97–3.60
Simonato et al. (1991)	0.40–0.79

5.1.2. Jones et al. (1988)

This study was an update of the cohort studied by Fox and Collier. Unfortunately, it does not provide as much information about duration of exposure, so the analysis must be limited to the autoclave workers. For those workers, four duration-of-employment categories are given (see their Table 4); in the present analysis estimated average durations of 1.5, 3, 7.5 and 15 years were used. Their Table 1 shows that the autoclave workers had exposures ranging between 150 and 800 ppm at various points in time. A value of 500 ppm was used in the PBPK model (8 h day^{-1}, 5 days $week^{-1}$) to get the average daily internal doses. The average daily internal doses were then multiplied by the four average durations of exposure to get four groups for analysis:

Cumulative dose	Obs.	Exp.
Low	0	0.07
Mid 1	1	0.08
Mid 2	2	0.08
High	4	0.15

The resulting risk estimates are shown in Table 5. The lower risk estimate was calculated using the value of P_0 derived in the Jones et al. (1988) study, while the higher risk estimate was calculated using an estimate of the lifetime liver cancer mortality rate in the US population (Chen and Blancato, 1989).

5.1.3. Simonato et al. (1991)

This study has the largest cohort and the most liver cancer deaths (24). Unfortunately, the exposure information may not be as accurate as in the other two studies discussed above, since it was collected from many different workplaces in several different countries, and since the original reporting of the exposure levels was relatively crude (ranges of < 50, 50–499, and ≥ 500 ppm). As in the Fox and Collier study, the classification was based on the 'highest level to which the workers were potentially exposed.' Thus, as with the previous studies, the estimates of risk from this cohort are probably underestimates of the true risk.

Another problem with the reporting of the results in this study is that the durations of exposure are not cross-classified according to exposure level as was done in the Fox and Collier report. In fact, there is very little information about duration of exposure that would allow estimation of an average value for the entire cohort, let alone the exposure groups. (Note that we cannot use the cumulative exposure groupings, as discussed above, because we need to have exposure level separated from exposure duration.) The information in Simonato et al. (1991) Table 2 (person years of observation by duration of employment) was used to estimate an average duration under the following assumption: if the follow-up time does not depend on the duration of employment, then the differences in the person-years of follow-up is due to the numbers of individuals in each duration category. The weighted average (trying different averages for the ≥ 20 year group) gives an estimate of 9 years of employment. This duration was used with model-predicted daily dose metrics for average exposure level estimates of 25, 158 and 600 ppm. The cumulative internal doses were input into the relative risk model with the following observed and expected liver cancer deaths:

Cumulative dose	Obs.	Exp.
Low cum. dose	4	2.52
Medium cum. dose	7	1.86
High cum. dose	12	2.12

The resulting risk estimates are shown in Table 5. Again, the lower risk estimate was calculated using the value of P_0 derived in the Simonato et al. (1991) study, while the higher risk estimate was calculated using an estimate of the lifetime liver cancer mortality rate in the US population (Chen and Blancato, 1989).

A comparison of the results of the analyses of the three sets of data, shown in Table 5, gives some indication of the consistency of the human results. The lifetime risk of liver cancer per ppm VC exposure estimated from the three studies only ranges over approximately one order of mag-

nitude: from 0.4×10^{-3} to 4.2×10^{-3}. Very similar risk estimates were also obtained with the alternative dose metrics (RISKM and RISKG). Moreover, these estimates are in remarkable agreement with the estimates based on animal data shown in Table 4. However, any confidence produced by this agreement should be tempered by the likelihood, discussed above, that misclassification of exposure in the human studies may somewhat underestimate the true risk at lower doses. Nevertheless, the agreement of the pharmacokinetic animal-based risk estimates with the pharmacokinetic human-based risk estimates provides strong support for the assumption used in this study: that cross-species scaling of lifetime cancer risk can be performed on a direct basis of lifetime average daily dose (without applying a body surface area adjustment) when the risks are based on biologically appropriate dose metrics calculated with a validated PBPK model.

6. Pharmacokinetic sensitivity / uncertainty analysis

Table 6 shows the normalized analytical sensitivities for the PBPK model used in this analysis. The normalized analytical sensitivity coefficient represents the fractional change in output associated with a fractional change in the input parameter. For example, if a 1% change in the input parameter results in a 2% change in the output, the sensitivity coefficient would be 2.0. In Table 6, the outputs are the dose metrics used in the analysis of angiosarcoma risk. The parameters in the table are defined in Tables 1 and 2. Sensitivity coefficients of less than 0.01 in absolute value were omitted from the table for clarity. None of the parameters display sensitivities significantly greater than 1.0, indicating that there is no amplification of error from the inputs to the

Table 6
Normalized parameter sensitivity in vinyl chloride PBPK model

Dose metric parameter	Rat gavage (11.9 mg kg^{-1}) Risk	Rat inhalation (50 ppm, 4 h) Risk	Human inhalation (1 ppm, continuous) Risk	Human drinking water (1 ppm) Risk
BW	−0.15	−0.26	−0.22	0.03
QPC	−0.08	0.32	0.11	−0.06
QCC	−0.06	0.65	0.44	−0.35
QFC	–	–	–	–
QLC	−0.06	0.64	0.44	−0.35
VFC	–	–	–	–
VLC	−1.03	−0.84	−0.66	−0.69
PB	0.09	0.73	0.88	0.09
PF	–	–	–	–
PS	–	–	–	–
PR	–	–	–	–
PL	–	–	–	–
VMAX1C	0.69	0.11	0.44	0.43
KM1	−0.07	−0.10	−0.44	−0.43
VMAX2C	0.06	–	–	–
KM2	−0.04	–	–	–
KA	0.29	–	–	–
KCO2C	–	–	–	–
KGSMC	–	–	–	–
KFEEC	–	–	–	–
GSO	–	–	–	–
KBC	–	–	–	–
KS	–	–	–	–
KOC	–	–	–	–

outputs. This is, of course, a desirable trait in a model to be used for risk assessment.

It can be seen that of the 24 parameters in the VC model, 10 have essentially no impact on risk predictions based on any of the dose metrics, and only eight have a significant impact on predictions based on RISK: the body weight (BW), alveolar ventilation (QPC), cardiac output (QCC), liver blood flow (QLC) and volume (VLC), blood/air partition coefficient (PB), the capacity (VMAX1C) and affinity (KM1) for metabolism by CYP2E1, and in the case of oral gavage, the oral uptake rate (KA). As discussed in the description of the PBPK model, all of these parameters could be reasonably well characterized from experimental data. However, the sensitivity of the risk predictions to the human values of these parameters implies that the risk from exposure to VC could vary considerably from individual to individual, depending on their specific physiology, level of activity, and metabolic capability.

The other dose metrics, RISKM and RISKG, are also sensitive to a number of the parameters in the model for the subsequent metabolism of the reactive metabolites, as well as for the GSH submodel (data not shown). Since these parameters could only be identified from data in rats, their values in the other species are uncertain. Given the sensitivity of RISKM and RISKG to these less certain parameters, and the general similarity of risks based on these two metrics to those based on the RISK metric, the use of the RISK metric would seem to be preferable for quantitative risk assessment.

6.1. Monte Carlo uncertainty / variability analysis

The sensitivity analysis described above does not consider the potential interactions between parameters; the parameters are tested individually. Also, sensitivity analysis does not adequately reflect the uncertainty associated with each parameter. The fact that the output is highly sensitive to a particular parameter is not important if the parameter is known exactly. To estimate the combined impact of uncertainty regarding the values of all the parameters, a Monte Carlo analysis can be performed. In a Monte Carlo analysis, the distributions of possible values for each of the input parameters are estimated. The Monte Carlo algorithm then randomly selects a value for each parameter from its distribution and runs the model. The random selection of parameter values and running of the model is repeated a large number of times (typically hundreds to thousands), until the distribution of the output has been characterized.

To assess the impact of parameter uncertainty on risk predictions, a dose–response model must be selected. In this case the linearized multistage model was used, for the reasons discussed earlier. The actual analysis was performed with our software package, PBPK_SIM, which was developed for the Air Force specifically to perform such a Monte Carlo analysis on PBPK models. The PBPK_SIM program randomly selects a set of parameter values from the distributions for the bioassay animal and runs the PBPK model to obtain dose metric values for each of the bioassay dose groups. It then selects a set of parameter values from the distributions for the human and runs the PBPK model to obtain a dose metric value for a specified human exposure scenario. Finally, it runs the linearized multistage model (or other specified risk model) with the animal and human dose metric values to obtain the human risk estimate. This entire process is repeated a specified number of times until the desired distribution of risks have been obtained.

Tables 1 and 2 list the means (preferred values) and coefficients of variation (CV) used in a Monte Carlo uncertainty analysis of the PBPK model. Truncated normal distributions were used for all parameters except the kinetic parameters, which were assumed to be lognormally distributed. The CVs for the physiological parameters were estimated from data on the variability of published values (USEPA, 1988; Lindstedt, 1992, personal communication), while the CVs for the partition coefficients were based on repeated determinations for two other chemicals, PERC (Gearhart et al., 1993) and chloropentafluorobenzene (Clewell and Jarnot, 1994). The CVs for the metabolic and kinetic constants were estimated from a comparison of reported values in the literature and by exercising the model against the various data sets

to determine the identifiability (i.e. whether changing the model parameters would effect the model fit to the data) of the parameters which were estimated from pharmacokinetic data.

The results of the Monte Carlo analysis are shown in Table 7, which lists the estimated risks associated with lifetime exposure to 1 ppm VC in air or 1 mg l^{-1} VC in drinking water (assuming a drinking water ingestion rate of 2 l day^{-1}). In all cases, the risk estimates represent the 95% UCL for risk, based on the LMS model. However, in order to characterize the impact of uncertainty in the pharmacokinetic parameters on the risk estimates, both the mean and the upper 95th percentile of the distribution of UCL risk estimates are shown. Thus, the mean value represents the best estimate of the pharmacokinetically-based upper-bound risk for VC exposure, and the 95th percentile provides a reasonable value for the 'highest probable' pharmacokinetic risk estimate, considering both pharmacokinetic uncertainty and uncertainty regarding the low-dose extrapolation. In general, the 95th percentiles of the distributions of risk estimates are within a factor of two of the means, indicating that pharmacokinetic uncertainty/variability is a relatively small contributor to the overall uncertainty in a risk assessment for VC.

7. Discussion

Giving priority to the animal studies most closely approximating the human route of exposure, the animal-based estimate of the carcinogenic risk of angiosarcoma from lifetime exposure to 1 ppm VC in air is 2.75×10^{-3}, or 1.1×10^{-6} μg^{-1} m^3, based on the geometric mean of the results shown in Table 4 for the inhalation studies with male and female rats and mice (Maltoni et al., 1981, 1984; Maltoni and Cotti, 1988). This value is consistent with the range of risk estimates from the epidemiological studies of 0.4×10^{-3} to 4.2×10^{-3} risk per ppm VC, but is roughly a factor of 80 below the inhalation unit risk of 8.4×10^{-5} μg^{-1} m^3 that has been used by the EPA since 1985 (Table 8). This difference is primarily attributable to the differences in cross-species scaling between the default approach and the pharmacokinetic approach. Similarly, the animal-based estimate of the carcinogenic risk of angiosarcoma from lifetime exposure to 1 μg l^{-1} VC in drinking water (assuming a drinking water ingestion rate of 2 l day^{-1}) is 6.8×10^{-7} $(\mu g\ l)^{-1}$, or 0.024 mg^{-1} kg day, based on the geometric mean of the results for the dietary administration of VC in male and female rats (Feron et al., 1981). This value is also roughly a factor of 80 below the unit risk of 1.9 mg^{-1} kg day, or 5.4×10^{-5} $(\mu g\ l)^{-1}$ that has been in use by the EPA since 1985. However, in this case the difference is primarily due to the use of the incidence of liver angiosarcoma alone in this analysis, as opposed to the total incidence of all liver tumors (angiosarcoma, hepatocellular carcinoma, hepatocellu-

Table 7
Mean and 95th percentile UCL risk/1000 for angiosarcoma based on the pharmacokinetic dose metric[a]

95% UCL risk/1000		1 ppm inhalation		1 mg/L drinking water	
Animal route	Sex/species	Mean/UCL	95th/UCL	Mean/UCL	95th/UCL
Inhalation	Male mouse	1.89	3.38	0.67	1.18
	Female mouse	3.89	6.95	1.39	2.33
Inhalation	Male rat	6.80	14.31	2.45	5.60
	Female rat	1.90	3.81	0.67	1.37
Oil gavage	Male rat	9.45	17.22	3.36	5.72
	Female rat	16.35	29.73	5.83	10.54
Diet	Male rat	3.26	5.26	1.14	1.64
	Female rat	1.15	1.87	0.41	0.60

[a] Dose metric, lifetime-average total amount metabolized per day, divided by volume of liver.

lar adenoma, and neoplastic lesions) plus lung angiosarcoma in the EPA risk assessment.

Although VC has often been cited as a chemical for which saturable metabolism should be considered in the risk assessment, saturation appears to become important only at very high exposure levels (greater than 250 ppm by inhalation or 25 mg kg^{-1} day^{-1} orally) compared to the lowest tumorigenic levels, and thus has little impact on the quantitative risk estimates. The important contribution of pharmacokinetic modeling is to provide a more biologically plausible estimate of the effective dose: total production of reactive metabolites in the target tissue. The ratio of this biologically effective dose to the administered dose is not uniform across routes and species. Therefore, any estimate of administered dose is less adequate for performing route-to-route and interspecies extrapolation of risk.

In the pharmacokinetic risk calculations presented in this report, no BSA adjustment factor was applied to obtain the human risks. Although this may appear to represent a departure from previous EPA practice in a risk assessment for VC, this marks the first time a pharmacokinetic dose metric has been used. The dose metric was selected to be consistent with the position stated in the interagency pharmacokinetics group consensus report on cross-species extrapolation of cancer (USEPA, 1992) that '...tissues experiencing equal average concentrations of the carcinogenic moiety over a full lifetime should be presumed to have equal lifetime cancer risk'. However, in the only pharmacokinetic risk assessment adopted by the EPA to this date, the pharmacokinetic dose metric used for methylene chloride was also a 'virtual concentration' of an as yet unidentified reactive metabolite, and its use similarly appeared to be consistent with the EPA position. Nevertheless, in their actual application of the methylene chloride pharmacokinetic model, EPA chose to adjust the pharmacokinetic dose metric by a BSA scaling factor to consider potential species differences in pharmacodynamics (USEPA, 1987).

The risk assessment performed in this study has focused on cancer risk from a continuous lifetime exposure, or at least an exposure over a large fraction of lifetime. Although there are certainly many uncertainties and unresolved issues regarding cross-species extrapolation of lifetime risks, there are even greater uncertainties regarding the extrapolation of partial-lifetime exposures. In particular, studies which have been performed with VC make it evident that extrapolation of partial lifetime exposure is not straightforward with this chemical. For example, in the comparative studies of partial lifetime exposure of rats to VC discussed earlier (Drew et al., 1983), while exposure from 0 to 6 months resulted in a similar tumor incidence to exposure from 6 to 12 months of life, exposure from 0 to 12 months produced a significantly different incidence than would be expected from the sum of the incidences for the two subintervals. For angiosarcomas, on the one hand, exposure to VC from 0 to 6 months and from 6 to 12 months resulted in incidences of 5.3 and 3.8%, respectively, while exposure from 0 to 12 months resulted in a much higher incidence of 21.4%. For hepatocellular carcinomas, on the other hand, exposure to VC from 0 to 6 months and from 6 to 12 months resulted in incidences of 4.0 and 11.5%, respectively, while exposure from 0 to 12 months resulted in an incidence of only 7.1%. Thus, this comparative bioassay does not provide support for a simple relationship of the observed incidence to the fraction of lifetime of the exposure. It seems reasonable to assume that newborns, with their higher rate of cell proliferation, should be at greater risk from genotoxic carcinogens, and some studies with VC support this assumption (Maltoni et al., 1981; Laib et al., 1989; Fedtke et al., 1990), although other well-conducted studies with VC do not (Drew et al.,

Table 8
Comparison of cancer risk estimates for vinyl chloride

Basis	Inhalation ($1\ \mu g/m^3$)	Drinking water ($1\ \mu g/l$)
Current EPA[a] HEAST Table (USEPA, 1997)	84.0×10^{-6}	54.0×10^{-6}
Pharmacokinetic model	1.1×10^{-6}	0.7×10^{-6}
Human epidemiology	$0.2\text{–}1.7 \times 10^{-6}$	

[a] Prior to publication of new EPA risk estimates based on this analysis.

1983). The issue of sensitive populations has never been seriously dealt with in quantitative carcinogenic risk assessment, but it would seem to be an appropriate consideration during risk management for specific potential exposures.

References

Agency for Toxic Substances and Disease Registry (ATSDR). 1993. Toxicological profile for vinyl chloride. U.S. Department of Health and Human Services, Public Health Service.

Andersen M, Clewell H, Gargas M, Smith FA, Reitz RH. Physiologically based pharmacokinetics and the risk assessment process for methylene chloride. Toxicol Appl Pharmacol 1987a;87:185–205.

Andersen ME, Gargas ML, Clewell HJ, Severyn KM. Quantitative evaluation of the metabolic interactions between trichloroethylene and 1,1-dichloroethylene by gas uptake methods. Toxicol Appl Pharmacol 1987b;89:149–157.

Astrand P, Rodahl K. Textbook of work physiology. New York: McGraw-Hill, 1970.

Baretta ED, Stewart RD, Mutchler JE. Monitoring exposures to vinyl chloride vapor: breath analysis and continuous air sampling. Am Ind Hyg Assoc J 1969;30:537–544.

Barton HA, Creech JA, Godin CS, Randall GM, Seckel CS. Chloroethylene mixtures: pharmacokinetic modeling and in vitro metabolism of vinyl chloride, trichloroethylene, and trans-1,2-dichloroethylene in the rat. Toxicol Appl Pharmacol 1995;130:237–247.

Bartsch H, Montesano R. Mutagenic and carcinogenic effects of vinyl chloride. Mutat Res 1975;32:93–114.

Bartsch H, Malaveille C, Montesano R. Human, rat and mouse liver-mediated mutagenicity of vinyl chloride in *S. typhimurium* strain. Int J Cancer 1975;15:429–437.

Bolt HM. Pharmacokinetics of vinyl chloride. Gen Pharmacol 1978;9:91–95.

Bolt HM, Kappus H, Buchter A, Bolt W. Disposition of [1,2-^{14}C]vinyl chloride in the rat. Arch Toxicol 1976;35:153–162.

Bolt HM, Laib RJ, Kappus H et al. Pharmacokinetics of vinyl chloride in the rat. Toxicology 1977;7:179–188.

Bolt HM, Laib RJ, Filser JG, Ottenwalder H, Buchter A. Vinyl chloride and related compounds: mechanisms of action on the liver. In: Berk, Chalmers, editors. Frontiers in liver disease, 1980.

Buchter A, Bolt HM, Filser JG, Goergens HW, Laib RJ, Bolt W. Pharmakokinetic und karzinogenese von vinylchlorid. Arbeitsmedizinische risikobeurteilung. Verhandlungen der deutchen gesellschaft fuer arbeitsmedizin, 18. Stuttgart: Gentner Verlag, 1978:111–124.

Buchter A, Filser JG, Peter H, Bolt HM. Pharmacokinetics of vinyl chloride in the Rhesus monkey. Toxicol Lett 1980;6:33–36.

Bull RJ, Brown JM, Meierhenry EA et al. Enhancement of the hepatotoxicity of chloroform in B6C3F1 mice by corn oil: implications for chloroform carcinogenesis. Environ Health Perspect 1986;69:49–58.

Byren D, Engholm G, Englund A et al. Mortality and cancer morbidity in a group of Swedish VCM and PVC workers. Environ Health Perspect 1976;17:167–170.

Chen CW, Blancato JN. Incorporation of biological information in cancer risk assessment: example — vinyl chloride. Cell Biol Toxicol 1989;5:417–444.

Cheng KC, Preston BD, Cahill DS, Dosanjh MK, Singer B, Loeb LA. The vinyl chloride DNA derivative N^2,3-ethenoguanine produces G → A transitions in *Escherichia coli*. Proc Natl Acad Sci 1991;88:9974–9978.

Clement Associates. 1987. Investigation of cancer risk assessment methods. Final report. Vol. 1: Introduction and epidemiology. Prepared for the U.S. Environmental Protection Agency, the Department of Defense, and the Electric Power Research Institute.

Clement International. 1990. Development and validation of methods for applying pharmacokinetic data in risk assessment. Final report. Volume V: Vinyl chloride. AAMRL-TR-90-072. Prepared for the Department of the Air Force, Armstrong Aerospace Medical Research Laboratory, Wright-Patterson Air Force Base, Ohio.

Clewell HJ, Jarnot BM. Incorporation of pharmacokinetics in non-carcinogenic risk assessment: example with chloropentafluorobenzene. Risk Anal 1994;14:265–276.

Creech JL, Johnson MN. Angiosarcoma of the liver in the manufacture of polyvinyl chloride. J Occup Med 1974;16:150–151.

DeAngelo AB, Daniel FB, McMillan L, Wernsing P, Savage RE. Species and strain sensitivity to the induction of peroxisome proliferation by chloroacetic acids. Toxicol Appl Pharmacol 1989;101:285–298.

Dosanjh JK, Chenna A, Kim E, Fraenkel-Conrat H, Samson L, Singer B. All four known cyclic adducts formed in DNA by the vinyl chloride metabolite chloroacetaldehyde are released by a human DNA glycosylase. Proc Natl Acad Sci 1994;91:1024–1028.

Drew RT, Boorman GA, Haseman JK et al. The effect of age and exposure duration on cancer induction by a known carcinogen in rats, mice, and hamsters. Toxicol Appl Pharmacol 1983;68:120–130.

D'Souza RW, Andersen ME. Physiologically based pharmacokinetic model for vinylidene chloride. Toxicol Appl Pharmacol 1988;95:230–240.

Fedtke N, Boucheron JA, Walker VE, Swenberg JA. Vinyl chloride-induced DNA adducts. II: Formation and persistence of 7-(2′-oxoethyl)guanine and N^2,3-ethenoguanine in rat tissue DNA. Carcinogenesis 1990;11:1287–1292.

Feron VJ, Hendriksen CFM, Speek AJ et al. Lifespan oral toxicity study of vinyl chloride in rats. Food Cosmet Toxicol 1981;19:317–333.

Filser JG, Bolt HM. Pharmacokinetics of halogenated ethylenes in rats. Arch Toxicol 1979;42:123–136.

Fox AJ, Collier PF. Mortality experience of workers exposure to vinyl chloride monomer in the manufacture of polyvinyl chloride in Great Britain. Br J Ind Med 1977;34:1–10.

Gargas ML, Andersen ME. Metabolism of inhaled brominated hydrocarbons: validation of gas uptake results by determination of a stable metabolite. Toxicol Appl Pharmacol 1982;66:55–68.

Gargas ML, Burgess RJ, Voisard DE, Cason GH, Andersen ME. Partition coefficients of low-molecular-weight volatile chemicals in various liquids and tissues. Toxicol Appl Pharmacol 1989;98:87–99.

Gargas ML, Clewell HJIII, Andersen ME. Gas uptake techniques and the rates of metabolism of chloromethanes, chloroethanes, and chloroethylenes in the rat. Inhal Toxicol 1990;2:295–319.

Gearhart JM, Mahle DA, Greene RJ, Seckel CS, Flemming CD, Fisher JW, Clewell HJ. Variability of physiologically based pharmacokinetic (PBPK) model parameters and their effect on PBPK model predictions in a risk assessment for perchloroethylene (PCE). Toxicol Lett 1993;68:131–144.

Gehring PJ, Watanabe PG, Park CN. Resolution of dose–response toxicity data for chemicals requiring metabolic activation: example — vinyl chloride. Toxicol Appl Pharmacol 1978;44:581–591.

Gehring PJ, Watanabe PG, Young JD. The relevance of dose-dependent pharmacokinetics in the assessment of carcinogenic hazard of chemicals. In: Book A, Hiatt HH, Watson JD, Winsten JA, editors. Origins of human cancer. Cold Spring Harbor, New York: Cold Spring Harbor Laboratory, 1977:187–203.

Green T, Hathway DE. Biological fate in rats of vinyl chloride in relation to its oncogenicity. Chem Biol Interact 1975;11(6):545–562.

Guengerich FP. Mammalian cytochromes P-450, vol. I. Boca Raton, FL: CRC Press, Inc, 1987.

Guengerich FP, Watanabe PG. Metabolism of [^{14}C]-labeled vinyl chloride in vivo and in vitro. Biochem Pharmacol 1979;28:589–596.

Guengerich FP, Strickland TW. Metabolism of vinyl chloride: destruction of the heme of highly purified liver microsomal cytochrome P-450 by a metabolite. Mol Pharmacol 1977;13:993–1004.

Guengerich FP, Kim D, Iwasaki M. Role of human cytochrome P-450 IIE1 in the oxidation of many low molecular weight cancer suspects. Chem Res Toxicol 1991; 4:168–179.

Hefner Jr. RE, Watanabe PG, Gehring PJ. Preliminary studies of the fate of inhaled vinyl chloride monomer in rats. Ann NY Acad Sci 1975;246:135–148.

Infante PF. Oncogenic and mutagenic risks in communities with polyvinyl chloride production facilities. Ann NY Acad Sci 1976;271:49–57.

Ivanetich KM, Aronson I, Katz ID. The interaction of vinyl chloride with rat hepatic microsomal cytochrome P-450 in vitro. Biochem Biophys Res Commun 1977;74:1411–1418.

Jaeger RJ, Murphy SD, Reynolds ES, Szabo S, Moslen MT. Chemical modification of acute hepatotoxicity of vinyl chloride monomer in rats. Toxicol Appl Pharmacol 1977;41:597–607.

Jedrychowski RA, Sokal JA, Chmielnicka J. Comparison of the impact of continuous and intermittent exposure to vinyl chloride, including phenobarbital effects. J Hyg Epidemiol Microbiol Immunol 1985;28:111–120.

Jedrychowski RA, Sokal JA, Chmielnicka J. Influence of exposure mode on vinyl chloride action. Arch Toxicol 1984;55:195–198.

Jones RW, Smith DM, Thomas PG. A mortality study of vinyl chloride monomer workers employed in the United Kingdom in 1940B1974. Scand J Work Environ Health 1988;14:153–160.

Laib RJ. The role of cyclic base adducts in vinyl-chloride-induced carcinogenesis: studies on nucleic acid alkylation in vivo, vol. 70. IARC Sci Publ, 1986:101–108.

Laib RJ, Bolt HM, Cartier R, Bartsch H. Increased alkylation of liver DNA and cell turnover in young versus old rats exposed to vinyl chloride correlates with cancer susceptibility. Toxicol Lett 1989;45:231–239.

Leibman KC. Current literature: metabolism of vinyl chloride. Drug Metab Disp 1977;5:93–94.

Lindstedt S. Personal communication — draft report to the ILSI RSI Physiological Parameters Working Group, 1992.

Malaveille C, Bartsch H, Barbin A et al. Mutagenicity of vinyl chloride, chloroethyleneoxide, chloroacetaldehyde, and chlorethanol. Biochem Biophys Res Commun 1975; 63:363–370.

Maltoni C, Cotti G. Carcinogenicity of vinyl chloride in Sprague–Dawley rats after prenatal and postnatal exposure. Ann NY Acad Sci 1988;534:145–159.

Maltoni C, Lefemine G, Ciliberti A et al. Carcinogenicity bioassay of vinyl chloride monomer: a model of risk assessment on an experimental basis. Environ Health Perspect 1981;41:3–29.

Maltoni C, Lefemine G, Ciliberti A et al. In: Maltoni C, Mehlman MA, editors. Experimental research on vinyl chloride carcinogenesis. Archives of research on industrial carcinogenesis, 2. Princeton, New Jersey: Princeton Scientific Publishers, Inc, 1984.

Monson RR, Peters JM, Johnson MN. Proportional mortality among vinyl chloride workers. Lancet 1974;2:397.

Nakajima T, Wang R, Elovaara E, Park SS, Gelboin HV, Vainio H. Cytochrome P450-related differences between rats and mice in the metabolism of benzene, toluene and trichloroethylene in liver microsomes. Biochem Pharmacol 1993;45:1079–1085.

National Cancer Institute (NCI). U.S. Cancer Mortality Rates and Trends 1950–1979. NCI/EPA Interagency Agreement on Environmental Carcinogenesis, 1983.

Newberne PM, Weigert J, Kula N. Effects of dietary fat on hepatic mixed function oxidases and hepatocellular carcinoma induced by aflatoxin B1 in rats. Cancer Res 1979;39:3986–3991.

Pepelko WE. Effect of exposure route on potency of carcinogens. Reg Toxicol Pharmacol 1991;13:3–17.

Pessayre D, Wandscheer JC, Descatoire V, Artigou JY, Benhamou JP. Formation and inactivation of a chemically reactive metabolite of vinyl chloride. Toxicol Appl Pharmacol 1979;49:505–515.

Pirastu R, Comba P, Reggiani A et al. Mortality from liver disease among Italian vinyl chloride monomer/polyvinyl chloride manufacturers. Am J Ind Med 1990;17:155–161.

Plugge H, Safe S. Vinylchloride metabolism — a review. Chemosphere 1977;6:309–325.

Purchase IFH, Stafford J, Paddle GM. Vinyl chloride — a cancer case study. In: Clayson D et al., editor. Toxicological risk assessment, II. Boca Raton, FL: CRC Press, 1985.

Ramsey JR, Andersen ME. A physiologically based description of the inhalation pharmacokinetics of styrene in rats and humans. Toxicol Appl Pharmacol 1984;73:159–175.

Rannug U, Johansson A, Ramel C et al. The mutagenicity of vinyl chloride after metabolic activation. Ambio 1974;3:194–197.

Reitz RH, Gargas ML, Anderson ME, Provan WF, Green T. Predicting cancer risk from vinyl chloride exposure with a physiologically based pharmacokinetic model. Toxicol Appl Pharmacol 1996;137:253–267.

Reitz RH, Mendrala AL, Guengerich FP. In vitro metabolism of methylene chloride in human and animal tissues: use in physiologically-based pharmacokinetic models. Toxicol Appl Pharmacol 1989;97:230–246.

Reynolds ES, Moslen MT, Szabo S, Jaeger RJ. Vinyl chloride-induced deactivation of cytochrome P-450 and other components of the liver mixed function oxidase system: an in vivo study. Res Commun Chem Pathol Pharmacol 1975;12:685–694.

Rinsky RA, Ott G, Water E et al. Study of mortality among chemical workers in the Kanawha Valley of West Virginia. Am J Ind Med 1988;13:429–438.

Sabadie N, Malaveille C, Carmus A-M, Bartsch H. Comparison of the hydroxylation of benzo[*a*]pyrene with the metabolism of vinyl chloride, *N*-nitrosomorpholine, and *N*-nitroso-'*N*'-methylpiperazine to mutagens by human and rat liver microsomal fractions,1980.

Simonato L, L'Abbe KA, Andersen A, Belli S, Comba P, Engholm G, Ferro G, Hagmar L, Langard S, Lundberg I, Pirastu R, Thomas P, Winkelmann R, Saracci R. A collaborative study of cancer incidence and mortality among vinyl chloride workers. Scand J Work Environ Health 1991;17:159–169.

Singer B. In vivo formation and persistence of modified nucleosides resulting from alkylating agents. Environ Health Perspect 1985;62:41–48.

Singer B, Spengler SJ, Chavez F, Kusmierek JT. The vinyl chloride-derived nucleoside, N^2,3-ethenoguanosine, is a highly efficient mutagen in transcription. Carcinogenesis 1987;8:745–747.

Swenberg JA, Fedtke N, Ciroussel F, Barbin A, Bartsch H. Etheno adducts formed in DNA of vinyl chloride-exposed rats are highly persistent in liver. Carcinogenesis 1992;13:727–729.

Tarkowski S, Wisniewska-Knypl JM, Klimczak J, Draminski W, Wroblewska K. Urinary excretion of thiodiglycolic acid and hepatic content of free thiols in rats at different levels of exposure to vinyl chloride. J Hyg Epidemiol Microbiol Immunol 1980;24:253–261.

Teta MJ, Schattner AR, Ott MG et al. Mortality surveillance in a large chemical company: the Union Carbide Corporation experience. Am J Ind Med 1990;17:435–448.

U.S. Environmental Protection Agency (USEPA). Health and environmental effects profile for chloroethane. Final draft. ECAO-CIN-P155. Prepared by Environmental Criteria and Assessment Office, Cincinnati, OH, 1985.

U.S. Environmental Protection Agency (USEPA). Update to the health assessment document and addendum for dichloromethane (methylene chloride): pharmacokinetics, mechanism of action, and epidemiology. External Review Draft. EPA/600/8-87/030A, 1987.

U.S. Environmental Protection Agency (USEPA). Reference physiological parameters in pharmacokinetic modeling. EPA/600/6-88/004. Office of Health and Environmental Assessment, Washington, DC, 1988

U.S. Environmental Protection Agency (USEPA). Request for comments on draft report of cross-species scaling factor for cancer risk assessment. Fed Reg 1992; 57: 24152.

U.S. Environmental Protection Agency (USEPA). Health Effects Assessment Summary Tables FY 1997 Update. EPA-540-R-97-036, Office of Solid Waste and Emergency Response, Washington, DC, 1997.

Van Duuren BL. Direct-acting alkylating and acylating agents. DNA adduct formation, structure-activity, and carcinogenesis. Annals New York Academy of Sciences, 1988:620–634.

Viola PL, Bigotti A, Caputo A. Oncogenic response of rats skin, lungs, and bones to vinyl chloride. Cancer Res 1971;31:516–522.

Walles SAS, Holmberg B, Svensson K, Osterman-Golkar S, Sigvardsson K, Lindblom K. Induction of single-strand breaks in liver DNA of mice after inhalation of vinyl chloride. IARC Sci Publ 1988;89:227–231.

Watanabe PG, Gehring PJ. Dose-dependent fate of vinyl chloride and its possible relationship to oncogenicity in rats. Environ Health Perspect 1976;17:145–152.

Watanabe PG, McGowan GR, Gehring PJ. Fate of ^{14}C-vinyl chloride after single oral administration in rats. Toxicol Appl Pharmacol 1976a;36(2):339–352.

Watanabe PG, Hefner RE, Gehring PJ. Fate of ^{14}C-vinyl chloride following inhalation exposure in rats. Toxicology 1976b;37:49–59.

Watanabe PG, Hefner RE, Gehring PJ. Vinyl chloride-induced depression of hepatic non-protein sulfhydryl content and effects on bromosulphalein (BSP) clearance in rats. Toxicology 1976c;6:1–8.

Watanabe PG, Zempel JA, Pegg DG, Gehring PJ. Hepatic macromolecular binding following exposure to vinyl chloride. Toxicol Appl Pharmacol 1978;44:571–579.

Waxweiler RJ, Stringer W, Wagoner JK et al. Neoplastic risk among workers exposed to vinyl chloride. Ann NY Acad Sci 1976;271:40–48.

Weber H, Reinl W, Greiser E. German investigations on morbidity and mortality of workers exposed to vinyl chloride. Environ Health Perspect 1981;41:95–99.

Withey JR. Pharmacodynamics and uptake of vinyl chloride monomer administered by various routes to rats. J Toxicol Environ Health 1976;1(3):381–394.

Wong O, Whorton MD, Ragland D, et al. An update of an epidemiologic study of vinyl chloride workers, 1942B1982. Prepared by Environmental Health Associates, Inc. for Chemical Manufacturers Association, 1986.

Wu W, Steenland K, Brown D et al. Cohort and case-control analyses of workers exposed to vinyl chloride: an update. J Occup Med 1989;31:518–523.

Message

From: Harvey Clewell [HClewell@ramboll.com]
Sent: 8/13/2018 9:37:48 PM
To: Schlosser, Paul [/o=ExchangeLabs/ou=Exchange Administrative Group (FYDIBOHF23SPDLT)/cn=Recipients/cn=121cf759d94e4f08afde0ceb646e711b-Schlosser, Paul]; Jerry Campbell [JCampbell@ramboll.com]; cvanlandingham@ramboll.com [/o=ExchangeLabs/ou=Exchange Administrative Group (FYDIBOHF23SPDLT)/cn=Recipients/cn=usereda39e51]
CC: Robinan Gentry [rgentry@ramboll.com]; Allison Franzen [AFranzen@ramboll.com]; Miyoung Yoon [myoon@toxstrategies.com]; Sonja Sax [SSax@ramboll.com]
Subject: RE: transmission of PBPK model for chloroprene

Hi Paul

Just to be clear, we did not adjust any PBPK model parameter to fit the in vivo dataset. QPC was measured in the study, and under the conditions of the in vivo exposure, V/Q matching requires that QPC/QCC be close to 1. I cannot support the use of a mouse value for QCC that is physiologically implausible.

Harvey Clewell
Principal Consultant

D +1 (919) 765-8025
M +1 (919) 4524279
hclewell@ramboll.com

From: Schlosser, Paul [mailto:Schlosser.Paul@epa.gov]
Sent: Monday, August 13, 2018 2:12 PM
To: Harvey Clewell <HClewell@ramboll.com>; Jerry Campbell <JCampbell@ramboll.com>; Cynthia Van Landingham <cvanlandingham@ramboll.com>
Cc: Robinan Gentry <rgentry@ramboll.com>; Allison Franzen <AFranzen@ramboll.com>; Miyoung Yoon <myoon@toxstrategies.com>; Sonja Sax <SSax@ramboll.com>
Subject: RE: transmission of PBPK model for chloroprene

Thanks, Harvey. Most of the corrections we are finding will likely have little impact, but the cumulative effect of making all of them can shift things a bit.

Two others not included in my previous email:

VLUC for the mouse should be 0.0073, instead of 0.007.

VRC: I replicated the calculations, which includes VLUC, but since the lung is a separate compartment, it's volume should not be included in these sums. So VRC needs to be reduced correspondingly for all 3 species.

Re. QCC for the mouse, I know there have been discussions about reported QCs being too low, but the fact that the mouse is being handled differently than the rat and human is an inconsistency. And if the human QPC reflects average daily activity, then the QCC should likewise be higher than 'resting'.

Adjusting a parameter to fit the in vivo PK data for a single data set (mouse) without an overall rationale, other supporting data (citations), and a means of knowing or predicting when such an adjustment should be used (hence, knowing what to do for humans), does not provide a model that can be reliably used for predicting human dosimetry based only on the in vitro PK and physiological data available.

-Paul

From: Harvey Clewell [mailto:HClewell@ramboll.com]
Sent: Monday, August 13, 2018 1:22 PM
To: Schlosser, Paul <Schlosser.Paul@epa.gov>; Jerry Campbell <JCampbell@ramboll.com>; cvanlandingham@ramboll.com
Cc: Robinan Gentry <rgentry@ramboll.com>; Allison Franzen <AFranzen@ramboll.com>; Miyoung Yoon <myoon@toxstrategies.com>; Sonja Sax <SSax@ramboll.com>
Subject: RE: transmission of PBPK model for chloroprene

Hi Paul

Here is the Partition Conversion sheet. I thought it was sent with the other documentation. In the process of double-checking it, we discovered that the value of the human liver:blood partition coefficient in Table 2 of Yang et al. (2012) is incorrect. Instead of 1.44 it should be 2.35, as calculated in the attached spreadsheet. Fortunately, this change does not significantly impact the dose metrics.

Harvey Clewell
Principal Consultant

D +1 (919) 765-8025
M +1 (919) 4524279
hclewell@ramboll.com

From: Schlosser, Paul [mailto:Schlosser.Paul@epa.gov]
Sent: Thursday, August 9, 2018 8:40 AM
To: Jerry Campbell <JCampbell@ramboll.com>; Cynthia Van Landingham <cvanlandingham@ramboll.com>; Harvey Clewell <HClewell@ramboll.com>
Cc: Robinan Gentry <rgentry@ramboll.com>; Allison Franzen <AFranzen@ramboll.com>; Miyoung Yoon <myoon@toxstrategies.com>; Sonja Sax <SSax@ramboll.com>
Subject: RE: transmission of PBPK model for chloroprene

Jerry, all,

In the 'Model Parameters' tab, listings for partition coefficients, the notes end with "See Partition Conversion sheet". There's no tab by that name.

Are you all developing a written report to go with this?

Alan Sasso has been able to rebuild the model, started mucking with it. I'll need another day or so. Alan was trying to figure out how the inputs (exposure control) works. So that may be where we want a walk-through.

-Paul

From: Jerry Campbell [mailto:JCampbell@ramboll.com]
Sent: Monday, August 06, 2018 9:30 AM
To: Schlosser, Paul <Schlosser.Paul@epa.gov>; cvanlandingham@ramboll.com; Harvey Clewell <HClewell@ramboll.com>
Cc: Robinan Gentry <rgentry@ramboll.com>; Allison Franzen <AFranzen@ramboll.com>; Miyoung Yoon <myoon@toxstrategies.com>; Sonja Sax <SSax@ramboll.com>
Subject: RE: transmission of PBPK model for chloroprene

I was just getting to that option. See if this will work.

Jerry Campbell
Managing Consultant

D 919-765-8022
jcampbell@ramboll.com

From: Schlosser, Paul [mailto:Schlosser.Paul@epa.gov]
Sent: Monday, August 06, 2018 9:26 AM
To: Cynthia Van Landingham <cvanlandingham@ramboll.com>; Harvey Clewell <HClewell@ramboll.com>
Cc: Robinan Gentry <rgentry@ramboll.com>; Allison Franzen <AFranzen@ramboll.com>; Jerry Campbell <JCampbell@ramboll.com>; Miyoung Yoon <myoon@toxstrategies.com>; Sonja Sax <SSax@ramboll.com>
Subject: RE: transmission of PBPK model for chloroprene

Try just changing the file-extension from .zip to .txt and sending as an attachment. I'm trying to unzip the thing from the sharepoint site and just getting a spinning wheel.

From: Cynthia Van Landingham [mailto:cvanlandingham@ramboll.com]
Sent: Monday, August 06, 2018 9:19 AM
To: Schlosser, Paul <Schlosser.Paul@epa.gov>; Harvey Clewell <HClewell@ramboll.com>
Cc: Robinan Gentry <rgentry@ramboll.com>; Allison Franzen <AFranzen@ramboll.com>; Jerry Campbell <JCampbell@ramboll.com>; Miyoung Yoon <myoon@toxstrategies.com>; Sonja Sax <SSax@ramboll.com>
Subject: RE: transmission of PBPK model for chloroprene

Unfortunately, I believe that the restrictions are on your end not ours. We can all see the files no problem.

Cynthia

Cynthia Van Landingham
Senior Managing Consultant

D +1 (318) 3982091
M +1 (318) 6147920
cvanlandingham@ramboll.com

From: Schlosser, Paul [mailto:Schlosser.Paul@epa.gov]
Sent: Monday, August 06, 2018 8:18 AM
To: Cynthia Van Landingham <cvanlandingham@ramboll.com>; Harvey Clewell <HClewell@ramboll.com>
Cc: Robinan Gentry <rgentry@ramboll.com>; Allison Franzen <AFranzen@ramboll.com>; Jerry Campbell <JCampbell@ramboll.com>; Miyoung Yoon <myoon@toxstrategies.com>; Sonja Sax <SSax@ramboll.com>
Subject: RE: transmission of PBPK model for chloroprene

I tried to just download it. Does it have to be this complicated? We'll be sharing with everyone as part of our open and transparent process…

-Paul

From: Cynthia Van Landingham [mailto:cvanlandingham@ramboll.com]
Sent: Monday, August 06, 2018 9:13 AM
To: Schlosser, Paul <Schlosser.Paul@epa.gov>; Harvey Clewell <HClewell@ramboll.com>
Cc: Robinan Gentry <rgentry@ramboll.com>; Allison Franzen <AFranzen@ramboll.com>; Jerry Campbell

<JCampbell@ramboll.com>; Miyoung Yoon <myoon@toxstrategies.com>; Sonja Sax <SSax@ramboll.com>
Subject: RE: transmission of PBPK model for chloroprene

Paul,

Did you download the zip file to your hard drive and then open or did you open it on the OneDrive site? If you did not try this, selecting all the files and allowing OneDrive to produce one download zip may be best. The chloroprene_model.o_error.txt file is not in the zip we created so may be something that is being created due to the download process. Please read that file to find out if your IT security set-up is preventing files from being extracted.

Thanks, Cynthia

Cynthia Van Landingham
Senior Managing Consultant

D +1 (318) 3982091
M +1 (318) 6147920
cvanlandingham@ramboll.com

From: Schlosser, Paul [mailto:Schlosser.Paul@epa.gov]
Sent: Monday, August 06, 2018 7:53 AM
To: Harvey Clewell <HClewell@ramboll.com>
Cc: Robinan Gentry <rgentry@ramboll.com>; Cynthia Van Landingham <cvanlandingham@ramboll.com>; Allison Franzen <AFranzen@ramboll.com>; Jerry Campbell <JCampbell@ramboll.com>; Miyoung Yoon <myoon@toxstrategies.com>; Sonja Sax <SSax@ramboll.com>
Subject: RE: transmission of PBPK model for chloroprene

Harvey,

I sent a separate email to Alison. Below is a screenshot of the model folder that I got. There are none of the scripts listed in the Excel 'documentation' file.

Once we have those, give us some time to look at it. Hopefully it's easy enough to figure out, but we can let you and Jerry know if we need a walk-through.

-Paul

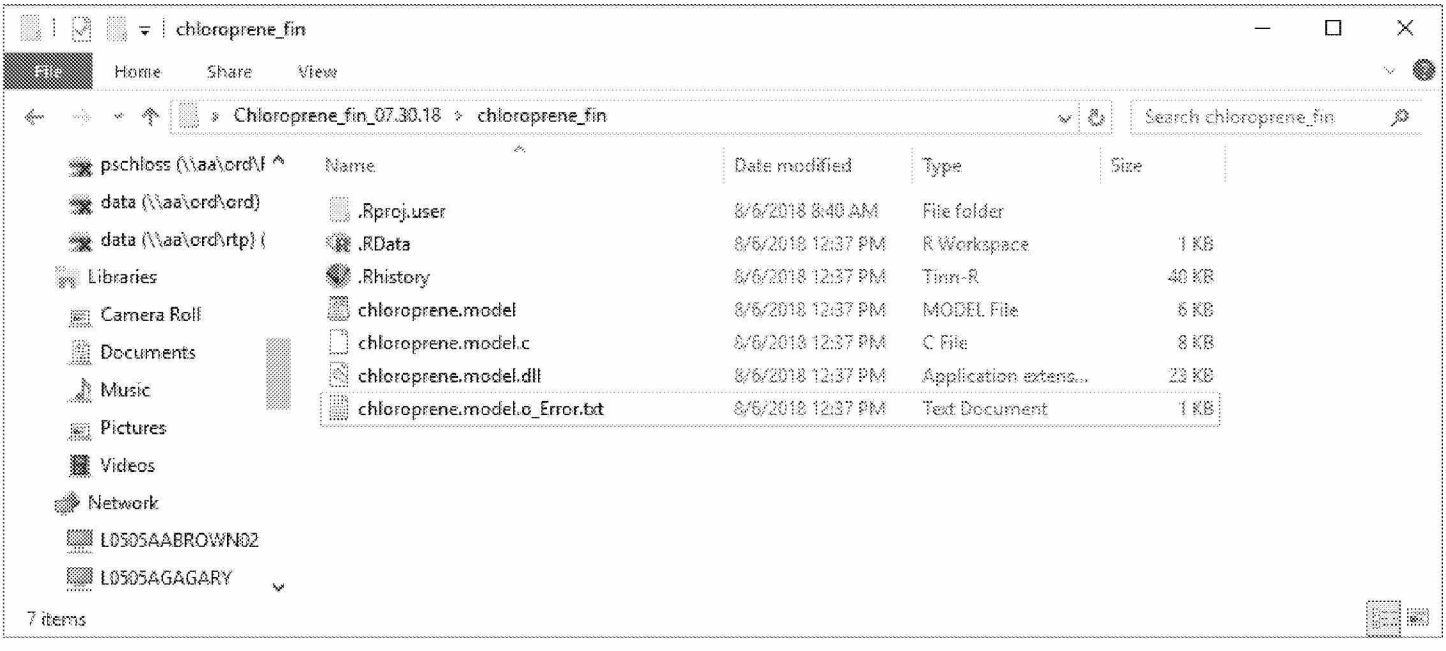

From: Harvey Clewell [mailto:HClewell@ramboll.com]
Sent: Friday, August 03, 2018 2:02 PM
To: Schlosser, Paul <Schlosser.Paul@epa.gov>
Cc: Robinan Gentry <rgentry@ramboll.com>; cvanlandingham@ramboll.com; Allison Franzen <AFranzen@ramboll.com>; Jerry Campbell <JCampbell@ramboll.com>; Miyoung Yoon <myoon@toxstrategies.com>; Sonja Sax <SSax@ramboll.com>
Subject: transmission of PBPK model for chloroprene

Hi Paul

As promised, we are providing you with the PBPK model for chloroprene written in R, with all the associated scripts and documentation. You should have received a separate email with an invitation to access the files on Microsoft OneDrive. Please let me if you have any problem downloading or opening them. Jerry Campbell would be happy to come over to EPA to help you set up the run environment in R studio and answer any questions you may have about running the model.

I'm looking forward to talking with you about the model and discussing any questions, suggestions, or concerns regarding it. Would it be possible to arrange an initial meeting sometime in the next few weeks. Miyoung Yoon is completing her review of the metabolism parameter scaling approach and I would like to be able to include you in the discussion of her recommendations.

Harvey Clewell

PhD, DABT, FATS
Principal Consultant
1692720 - Tampa

D +1 (919) 765-8025
M +1 (919) 4524279
hclewell@ramboll.com

Connect with us

Ramboll
6 Davis Drive
Suite 139
PO Box 13441
Research Triangle Park
NC 27709
USA
www.ramboll.com

Message

From: Harvey Clewell [HClewell@ramboll.com]
Sent: 8/13/2018 5:21:51 PM
To: Schlosser, Paul [/o=ExchangeLabs/ou=Exchange Administrative Group (FYDIBOHF23SPDLT)/cn=Recipients/cn=121cf759d94e4f08afde0ceb646e711b-Schlosser, Paul]; Jerry Campbell [JCampbell@ramboll.com]; cvanlandingham@ramboll.com [/o=ExchangeLabs/ou=Exchange Administrative Group (FYDIBOHF23SPDLT)/cn=Recipients/cn=usereda39e51]
CC: Robinan Gentry [rgentry@ramboll.com]; Allison Franzen [AFranzen@ramboll.com]; Miyoung Yoon [myoon@toxstrategies.com]; Sonja Sax [SSax@ramboll.com]
Subject: RE: transmission of PBPK model for chloroprene
Attachments: PC calculations.xlsx

Hi Paul

Here is the Partition Conversion sheet. I thought it was sent with the other documentation. In the process of double-checking it, we discovered that the value of the human liver:blood partition coefficient in Table 2 of Yang et al. (2012) is incorrect. Instead of 1.44 it should be 2.35, as calculated in the attached spreadsheet. Fortunately, this change does not significantly impact the dose metrics.

Harvey Clewell
Principal Consultant

D +1 (919) 765-8025
M +1 (919) 4524279
hclewell@ramboll.com

From: Schlosser, Paul [mailto:Schlosser.Paul@epa.gov]
Sent: Thursday, August 9, 2018 8:40 AM
To: Jerry Campbell <JCampbell@ramboll.com>; Cynthia Van Landingham <cvanlandingham@ramboll.com>; Harvey Clewell <HClewell@ramboll.com>
Cc: Robinan Gentry <rgentry@ramboll.com>; Allison Franzen <AFranzen@ramboll.com>; Miyoung Yoon <myoon@toxstrategies.com>; Sonja Sax <SSax@ramboll.com>
Subject: RE: transmission of PBPK model for chloroprene

Jerry, all,

In the 'Model Parameters' tab, listings for partition coefficients, the notes end with "See Partition Conversion sheet". There's no tab by that name.

Are you all developing a written report to go with this?

Alan Sasso has been able to rebuild the model, started mucking with it. I'll need another day or so. Alan was trying to figure out how the inputs (exposure control) works. So that may be where we want a walk-through.

-Paul

From: Jerry Campbell [mailto:JCampbell@ramboll.com]
Sent: Monday, August 06, 2018 9:30 AM
To: Schlosser, Paul <Schlosser.Paul@epa.gov>; cvanlandingham@ramboll.com; Harvey Clewell <HClewell@ramboll.com>
Cc: Robinan Gentry <rgentry@ramboll.com>; Allison Franzen <AFranzen@ramboll.com>; Miyoung Yoon

<myoon@toxstrategies.com>; Sonja Sax <SSax@ramboll.com>
Subject: RE: transmission of PBPK model for chloroprene

I was just getting to that option. See if this will work.

Jerry Campbell
Managing Consultant

D 919-765-8022
jcampbell@ramboll.com

From: Schlosser, Paul [mailto:Schlosser.Paul@epa.gov]
Sent: Monday, August 06, 2018 9:26 AM
To: Cynthia Van Landingham <cvanlandingham@ramboll.com>; Harvey Clewell <HClewell@ramboll.com>
Cc: Robinan Gentry <rgentry@ramboll.com>; Allison Franzen <AFranzen@ramboll.com>; Jerry Campbell <JCampbell@ramboll.com>; Miyoung Yoon <myoon@toxstrategies.com>; Sonja Sax <SSax@ramboll.com>
Subject: RE: transmission of PBPK model for chloroprene

Try just changing the file-extension from .zip to .txt and sending as an attachment. I'm trying to unzip the thing from the sharepoint site and just getting a spinning wheel.

From: Cynthia Van Landingham [mailto:cvanlandingham@ramboll.com]
Sent: Monday, August 06, 2018 9:19 AM
To: Schlosser, Paul <Schlosser.Paul@epa.gov>; Harvey Clewell <HClewell@ramboll.com>
Cc: Robinan Gentry <rgentry@ramboll.com>; Allison Franzen <AFranzen@ramboll.com>; Jerry Campbell <JCampbell@ramboll.com>; Miyoung Yoon <myoon@toxstrategies.com>; Sonja Sax <SSax@ramboll.com>
Subject: RE: transmission of PBPK model for chloroprene

Unfortunately, I believe that the restrictions are on your end not ours. We can all see the files no problem.

Cynthia

Cynthia Van Landingham
Senior Managing Consultant

D +1 (318) 3982091
M +1 (318) 6147920
cvanlandingham@ramboll.com

From: Schlosser, Paul [mailto:Schlosser.Paul@epa.gov]
Sent: Monday, August 06, 2018 8:18 AM
To: Cynthia Van Landingham <cvanlandingham@ramboll.com>; Harvey Clewell <HClewell@ramboll.com>
Cc: Robinan Gentry <rgentry@ramboll.com>; Allison Franzen <AFranzen@ramboll.com>; Jerry Campbell <JCampbell@ramboll.com>; Miyoung Yoon <myoon@toxstrategies.com>; Sonja Sax <SSax@ramboll.com>
Subject: RE: transmission of PBPK model for chloroprene

I tried to just download it. Does it have to be this complicated? We'll be sharing with everyone as part of our open and transparent process…

-Paul

From: Cynthia Van Landingham [mailto:cvanlandingham@ramboll.com]
Sent: Monday, August 06, 2018 9:13 AM
To: Schlosser, Paul <Schlosser.Paul@epa.gov>; Harvey Clewell <HClewell@ramboll.com>
Cc: Robinan Gentry <rgentry@ramboll.com>; Allison Franzen <AFranzen@ramboll.com>; Jerry Campbell <JCampbell@ramboll.com>; Miyoung Yoon <myoon@toxstrategies.com>; Sonja Sax <SSax@ramboll.com>
Subject: RE: transmission of PBPK model for chloroprene

Paul,

Did you download the zip file to your hard drive and then open or did you open it on the OneDrive site? If you did not try this, selecting all the files and allowing OneDrive to produce one download zip may be best. The chloroprene_model.o_error.txt file is not in the zip we created so may be something that is being created due to the download process. Please read that file to find out if your IT security set-up is preventing files from being extracted.

Thanks, Cynthia

Cynthia Van Landingham
Senior Managing Consultant

D +1 (318) 3982091
M +1 (318) 6147920
cvanlandingham@ramboll.com

From: Schlosser, Paul [mailto:Schlosser.Paul@epa.gov]
Sent: Monday, August 06, 2018 7:53 AM
To: Harvey Clewell <HClewell@ramboll.com>
Cc: Robinan Gentry <rgentry@ramboll.com>; Cynthia Van Landingham <cvanlandingham@ramboll.com>; Allison Franzen <AFranzen@ramboll.com>; Jerry Campbell <JCampbell@ramboll.com>; Miyoung Yoon <myoon@toxstrategies.com>; Sonja Sax <SSax@ramboll.com>
Subject: RE: transmission of PBPK model for chloroprene

Harvey,

I sent a separate email to Alison. Below is a screenshot of the model folder that I got. There are none of the scripts listed in the Excel 'documentation' file.

Once we have those, give us some time to look at it. Hopefully it's easy enough to figure out, but we can let you and Jerry know if we need a walk-through.

-Paul